A GDI (AGS3) and a GEF (GIV) regulate autophagy by balancing G protein activity and growth factor signals

Mikel Garcia-Marcos[a,*], Jason Ear[b], Marilyn G. Farquhar[a], and Pradipta Ghosh[a,b,*]
Departments of [a]Cellular and Molecular Medicine and [b]Medicine, School of Medicine, University of California, San Diego, La Jolla, CA 92093

ABSTRACT **Autophagy is the major catabolic process responsible for the removal of aggregated proteins and damaged organelles. Autophagy is regulated by both G proteins and growth factors, but the underlying mechanism of how they are coordinated during initiation and reversal of autophagy is unknown. Using protein–protein interaction assays, G protein enzymology, and morphological analysis, we demonstrate here that Gα-interacting, vesicle-associated protein (GIV, a.k.a. Girdin), a nonreceptor guanine nucleotide exchange factor for $G\alpha_{i3}$, plays a key role in regulating autophagy and that dynamic interplay between $G\alpha_{i3}$, activator of G-protein signaling 3 (AGS3, its guanine nucleotide dissociation inhibitor), and GIV determines whether autophagy is promoted or inhibited. We found that AGS3 directly binds light chain 3 (LC3), recruits $G\alpha_{i3}$ to LC3-positive membranes upon starvation, and promotes autophagy by inhibiting the G protein. Upon growth factor stimulation, GIV disrupts the $G\alpha_{i3}$–AGS3 complex, releases $G\alpha_{i3}$ from LC3-positive membranes, enhances anti-autophagic signaling pathways, and inhibits autophagy by activating the G protein. These results provide mechanistic insights into how reversible modulation of $G\alpha_{i3}$ activity by AGS3 and GIV maintains the delicate equilibrium between promotion and inhibition of autophagy.**

Monitoring Editor
Tamotsu Yoshimori
Osaka University

Received: Sep 1, 2010
Revised: Dec 1, 2010
Accepted: Dec 20, 2010

INTRODUCTION

Autophagy is an adaptive response to unfavorable conditions, such as nutrient deprivation, that result in degradation of cellular components. Thus autophagy maintains cellular homeostasis by balancing biosynthesis and degradation. In addition to its role in organelle turnover, development, and aging (Cecconi and Levine, 2008), dysregulation of autophagy is a key pathophysiologic component of many diseases, such as cancer, neurodegeneration, cardiovascular disorders, and microbial invasion (reviewed in Shintani and Klionsky, 2004; Levine and Kroemer, 2008). Paradoxically, autophagy has both beneficial and deleterious effects in many of these disorders (Shintani and Klionsky, 2004), which highlights the importance of tight regulation of the various pro- and anti-autophagic signaling pathways that maintain levels of autophagy in a delicate equilibrium.

Both growth factor– and G protein–mediated signaling pathways appear to be involved in the maintenance of this equilibrium. The role of growth factor–mediated signaling as a major regulator of autophagy has been unequivocally established (Lum *et al.*, 2005): Insulin and insulin-like growth factor stimulation activates the phosphoinositide 3-kinase (PI3K)–Akt pathway, leading to increased activation of mammalian target of rapamycin (mTOR), which inhibits autophagy (Beugnet *et al.*, 2003; Meijer and Codogno, 2004). Heterotrimeric G proteins also regulate autophagy (Ogier-Denis *et al.*, 1995, 1996, 2000; Pattingre *et al.*, 2003; Gohla *et al.*, 2007): Active, guanosine 5′-triphosphate (GTP)–bound $G\alpha_{i3}$ inhibits starvation-induced

This article was published online ahead of print in MBoC in Press (http://www.molbiolcell.org/cgi/doi/10.1091/mbc.E10-08-0738) on January 5, 2011.

*These authors contributed equally to this work.

Address correspondence to: Pradipta Ghosh (prghosh@ucsd.edu) and Mikel Garcia-Marcos (mgarciamarcos@ucsd.edu).

Abbreviations used: AGS3, activator of G-protein signaling 3; CT, C terminus; DAPI, 4′,6-diamino-2-phenylindole; DTT, dithiothreitol; EGFR, epidermal growth factor receptor; EM, electron microscopy; ER, endoplasmic reticulum; ERK, extracellular signal–regulated kinase; FBS, fetal bovine serum; FCS, fetal calf serum; GAP, GTPase activating protein; GDI, guanine nucleotide dissociation inhibitor; GDP, guanosine 5′-diphosphate; GEF, guanine nucleotide exchange factor; GFP, green fluorescent protein; GIV, Gα-interacting, vesicle-associated protein; GIV-FA, GIV F1685A mutant; GoLoco, $G\alpha_{i/o}$-Loco; GPCR, G protein–coupled receptor; GTP, guanosine 5′-triphosphate; HBSS, Hank's balanced salt solution; IB, immunoblotting; IgG, immunoglobulin G; LC3, light chain 3; mAb, monoclonal antibody; mTOR, mammalian target of rapamycin; NA, numerical aperture; pAb, polyclonal antibody; pERK1/2, phospho-extracellular signal–regulated kinase 1/2; PI3K, phosphoinositide 3-kinase; PM, plasma membrane; S6K, ribosomal protein S6 kinase; siRNA, small interfering RNA; WT, wild-type.

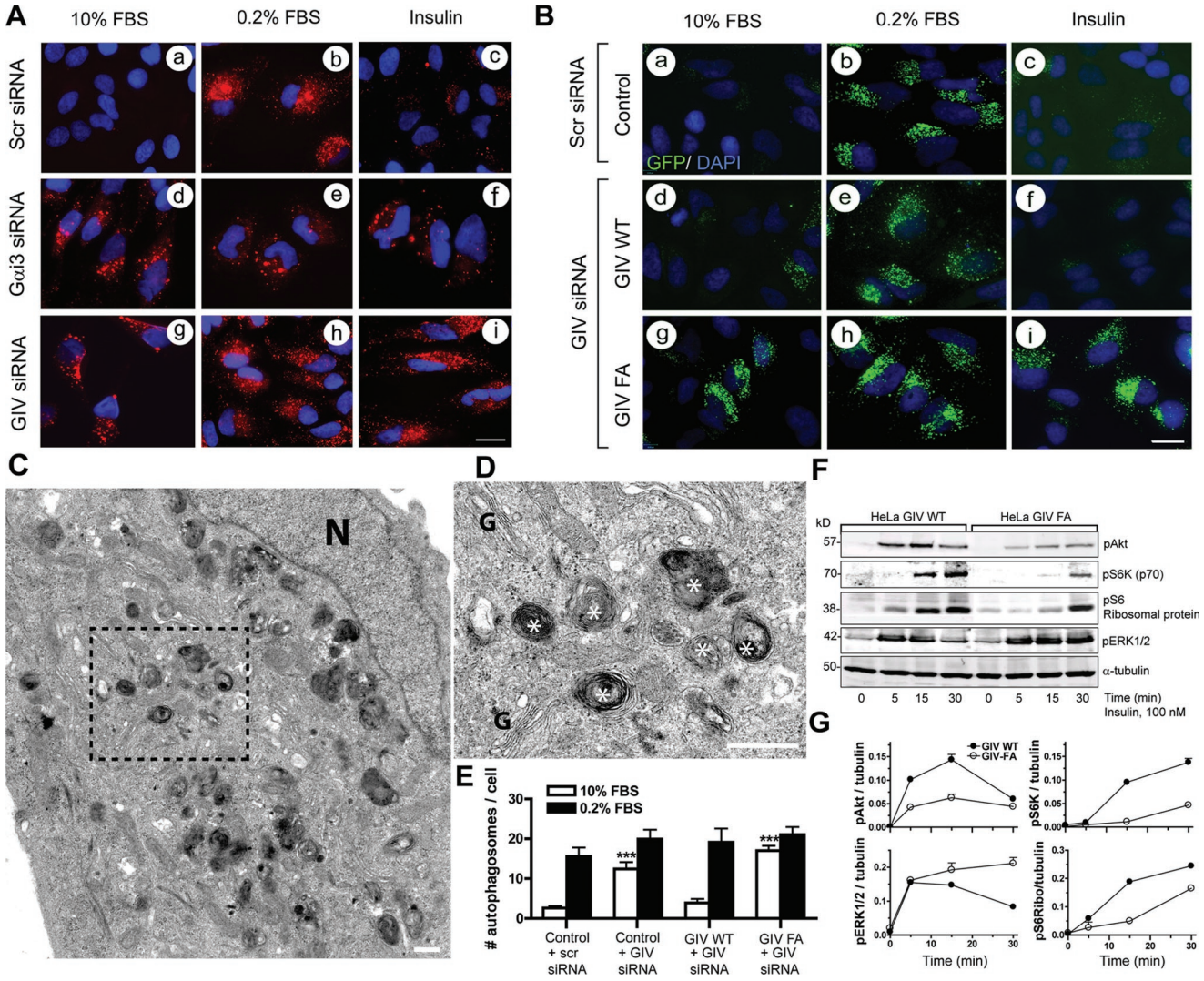

FIGURE 1: GIV inhibits autophagy via its GEF motif. (A) $G\alpha_{i3}$ and GIV are required for insulin-mediated reversal of autophagy. HeLa cells were treated with previously validated (Ghosh *et al.*, 2008) scrambled (Scr, a–c), $G\alpha_{i3}$ (d–f), or GIV (g–i) siRNA oligos for 48 h, after which they were either maintained in 10% FBS, serum starved for 8 h in 0.2% FBS, or serum starved for 8 h and then treated with 100 nM insulin for 1 h. They were then fixed, stained for LC3 (red) and the nucleus/DAPI (blue), and analyzed by confocal microscopy. Scr-treated controls showed little or no vesicular LC3 staining in 10% FBS (a), increased numbers of LC3-positive vesicles upon serum starvation (b), and disappearance of LC3-positive vesicles upon insulin treatment (c). Depletion of both $G\alpha_{i3}$ and GIV was accompanied by increased LC3-positive vesicles in 10% FBS (d, g) as well as when serum starved (e, h), with persistence of staining despite insulin treatment (f, i). Efficient depletion of $G\alpha_{i3}$ (~85–95%) and GIV (~80–90%) was confirmed by immunoblotting (IB) (Supplemental Figure S1A). Bar = 10 μM. (B) Insulin reverses autophagy in GIV-WT, but not in the GEF-deficient GIV-FA cells, as determined by changes in the localization of GFP-LC3. Untransfected HeLa cells (control) or HeLa cells stably expressing either siRNA-resistant wild-type GIV (GIV-WT) or GEF-deficient GIV (GIV-FA) were first treated with scrambled (Scr) or GIV siRNA followed by transient transfection with GFP-LC3. Cells were subsequently serum starved or treated with insulin as in (A) and then fixed and stained with DAPI (blue) and analyzed by fluorescence microscopy. Scr-treated controls and GIV-WT cells show little or no vesicular GFP-LC3 staining (green) at steady state when grown in 10% FBS (a, d), increased GFP-LC3–positive vesicles upon serum starvation (b, e), and virtual disappearance of GFP-LC3–positive vesicles upon insulin treatment (c, f). GIV-FA cells show increased GFP-LC3–positive vesicles at steady state (g) and upon serum starvation (h), and persistence of GFP-LC3–positive vesicular staining after insulin treatment (i) compared with controls. Efficient depletion (~85–90%) of GIV (Supplemental Figure S1B) and transfection of GFP-LC3 (~80–90%, unpublished data) were confirmed by IB. Bar = 10 μM. (C–E) Quantitative and qualitative assessment of autophagy by electron microscopy (EM). Control, GIV-WT, and GIV-FA cells were treated with scrambled (Scr) or GIV siRNA as in (B) and (Figure S1B), fixed, and examined by EM. Autophagosomal structures (white asterisks) were counted in randomly selected fields (~40 per sample) where the section cut through the Golgi stack (G) and nucleus (N). The size of most autolysosomal structures ranged from 0.5 to 1.5 μM in diameter, and some complex forms measuring up to 4 μM were seen occasionally. The average size of autophagic structures did not vary significantly between samples. (C) EM micrograph of a representative field from GIV-FA cells maintained in the presence of 10% serum. Boxed area in (C) is enlarged in (D) to show a higher magnification view of a cluster of autophagosomes. Similar autophagosomes were found in control, GIV-WT, and GIV-FA cells upon serum starvation. Bar graphs (E) showing the average number of

autophagy whereas inactive, guanosine 5′-diphosphate (GDP)–bound $G\alpha_{i3}$ stimulates autophagy (Ogier-Denis *et al.*, 1995, 1996). Consistent with this, both activator of G-protein signaling 3 (AGS3), a guanine nucleotide dissociation inhibitor (GDI) that keeps Gi in an inactive state (Pattingre *et al.*, 2003), and GAIP/RGS19, a GTPase activating protein (GAP) that inactivates Gi (Ogier-Denis *et al.*, 1997), promote autophagy. Recent reports demonstrate that $G\alpha_{i3}$ is required for the anti-autophagic action of insulin (Gohla *et al.*, 2007) and for the enhancement of the anti-autophagic Akt-mTOR pathway by other growth factors (Cao *et al.*, 2009). Although these findings suggest that growth factor signaling and G protein activity are intertwined in the regulation of autophagy, little is known about the precise molecular mechanisms that regulate this interplay. What activates the G protein and how growth factor signaling influences this activation step during autophagy have remained a mystery.

We recently reported that Gα-interacting, vesicle-associated protein (GIV or Girdin), a nonreceptor guanine nucleotide exchange factor (GEF) for $G\alpha_{i3}$ (Garcia-Marcos *et al.*, 2009), operates at the interface between growth factor and G protein signaling (Ghosh *et al.*, 2010). By linking G proteins to ligand-activated epidermal growth factor receptor (EGFR), GIV reprograms EGF signaling to specifically enhance PI3K-Akt signals from the plasma membrane (PM) (Ghosh *et al.*, 2010). Because PI3K-Akt signals and G protein activation are two major triggers for the regulation of autophagy (Meijer and Codogno, 2004) and GIV operates at the crossroads of both, we investigated whether activation of Gi by GIV influences autophagy.

RESULTS

GIV inhibits autophagy and is required for the anti-autophagic action of insulin

To investigate whether GIV plays a role in autophagy, we depleted HeLa cells of endogenous GIV or $G\alpha_{i3}$ (Supplemental Figure S1A) and assessed autophagic activity by immunofluorescence after staining for endogenous light chain 3 (LC3), a well-established effector of autophagy as well as a bona fide marker for autophagosomes (Klionsky *et al.*, 2008; Kimura *et al.*, 2009). Punctate LC3 staining provides a measure of ongoing autophagy because it marks the successful processing of a cytosolic form, LC3-I, to LC3-II, a phospholipid conjugated form that is targeted to preautophagosomal and autophagosomal membranes (Mizushima and Yoshimori, 2007; Kimura *et al.*, 2009). We chose to induce autophagy by starving cells in serum-free media because previous studies have established that GIV is required for signal transduction by a variety of growth factors (Ghosh *et al.*, 2008, 2010; Jiang *et al.*, 2008; Kitamura *et al.*, 2008; Garcia-Marcos *et al.*, 2009). In control cells, punctate LC3 staining was infrequently seen when cells were maintained in 10% fetal bovine serum (FBS), markedly induced when the cells were starved, and virtually abolished when starved cells were stimulated for 1 h with insulin (Figure 1A, a–c). By contrast, in cells depleted of endogenous GIV large numbers of LC3-positive puncta were observed in the presence of 10% FBS as well as upon starvation, and such staining persisted even after insulin stimulation (Figure 1A, g–i). Virtually identical results were obtained in cells depleted of endogenous $G\alpha_{i3}$ (Figure 1A, d–f), the major $G\alpha_i$-type subunit expressed in HeLa cells (Krumins and Gilman, 2006) and the only $G\alpha_i$ involved in autophagy (Ogier-Denis *et al.*, 1995; Gohla *et al.*, 2007). These differences in the abundance of autophagosomes suggest that without $G\alpha_{i3}$ or GIV the level of autophagy is increased under nutrient-rich conditions and that cells are rendered unresponsive to the anti-autophagic actions of insulin.

GIV inhibits autophagy via its GEF function

To discern whether activation of Gi by GIV is the basis for GIV's role in the anti-autophagic action of insulin, we used a set of previously characterized (Garcia-Marcos *et al.*, 2009; Ghosh *et al.*, 2010) HeLa cell lines stably expressing either siRNA-resistant wild-type GIV (GIV-WT cells) or GEF-deficient GIV F1685A mutant (GIV-FA) cells incapable of activating the G protein. GIV-WT and GIV-FA cells were depleted of endogenous GIV using GIV siRNA, parental (hereby referred to as control) HeLa cells were treated with scrambled siRNA (Supplemental Figure S1B), and all cell lines were transfected with green fluorescent protein (GFP)–LC3. The levels of autophagy at steady state (10% FBS), upon starvation (0.2% FBS), or after insulin stimulation were compared by immunofluorescence. In control cells punctate GFP-LC3 staining was observed in serum-starved cells but not in cells maintained in 10% FBS or in cells stimulated with insulin (Figure 1B, a–c). This pattern of staining was similar to that seen with endogenous LC3 (Figure 1A, a–c), thus validating the use of the GFP-tagged protein as a readout for autophagy. In GIV-WT cells few GFP-LC3–positive puncta were seen when cells were maintained in 10% FBS, many upon starvation, and virtually none after stimulation of starved cells with insulin (Figure 1B, d–f), whereas in GIV-FA cells high levels of GFP-LC3–positive puncta were seen regardless of whether the cells were grown in the presence of serum or insulin (Figure 1A, d–f). Identical results were obtained when we immunostained for endogenous LC3 in GIV-WT and GIV-FA cells (Supplemental Figure S2). We also verified that the increased numbers of GFP-LC3–positive structures seen in GIV-FA cells were not due to impaired maturation because they colocalize with cathepsin D, indicative of successful maturation into autolysosomes (Supplemental Figure S3). Taken together, these results indicate that autophagy is promoted when GIV cannot bind or activate $G\alpha_{i3}$. We conclude that GIV, and, more specifically, its GEF function, is required to inhibit autophagy and that in its absence autophagy is inhibited even in the presence of nutrients and growth factors.

autophagosomal structures/cell profile in each cell line in the presence of serum (10% FBS) or serum starved (0.2% FBS). Results are shown as mean ± SEM (n = 10). *** denotes p value < 0.001. Results from one of three independent experiments are displayed. Bar = 1 μM. (F, G) GIV-WT cells show enhanced Akt and mTOR signaling and suppressed ERK1/2 signaling in response to insulin, whereas GIV-FA cells show the opposite signaling profile. (F) GIV-WT and GIV-FA HeLa cells depleted of endogenous GIV (GIV siRNA) were serum starved as in (A), stimulated with 100 nM insulin for different times (5, 15, and 30 min), and cell lysates were analyzed for phospho (p) Akt, pS6K (p70), pS6 ribosomal protein, pERK1/2, and tubulin by IB. (G) The kinetics of insulin-initiated signaling pathways in HeLa cell lines were determined (phosphoprotein:tubulin ratios) at each time point after insulin stimulation and expressed as fold increase in activation normalized to t = 0 min. Peak phosphorylation of Akt, S6K, and S6 ribosomal protein is significantly higher in GIV-WT (at 15 min) compared with GIV-FA cells, whereas both cell lines achieved similar enhancement of ERK1/2 phosphorylation at 5 min. Phosphorylation of ERK1/2 was sustained in GIV-FA but reduced in GIV-WT cells by 30 min. Results are shown as mean ± SEM (n = 3); p < 0.05 for GIV-WT vs. GIV-FA at 15 min for all phosphoproteins analyzed. Significant differences persist at 30 min for pS6K and pERK1/2.

Because assessment of LC3 processing by immunoblotting is unreliable in HeLa cells (Klionsky *et al.*, 2008), we used morphological analysis by electron microscopy (EM) as a well-established alternative approach (Klionsky *et al.*, 2008) to assess cellular autophagy. We minimized sampling artifacts by establishing a consistent basis for identification and quantification of autophagic elements (see *Materials and Methods*). When cells were serum starved, numerous vesicles with multilamellar intraluminal contents representing various stages of autophagy and ranging from 0.5 to 1.5 μM in diameter were seen in all cell lines (Figure 1, C and D). When grown in the presence of 10% serum, scrambled siRNA–treated control HeLa cells and HeLa GIV-WT cells showed very few autophagosomes, whereas large numbers of autophagosomes were seen in both GIV-depleted HeLa cells and GIV-FA cells (Figure 1E). These results indicate that in the presence of growth factors (those present in serum in this case) GIV's GEF function is required for effective inhibition of autophagy.

GIV's GEF function enhances anti-autophagic Akt-mTOR signals

We previously demonstrated that GIV's GEF function is required for Akt enhancement in response to insulin (Ghosh *et al.*, 2008; Garcia-Marcos *et al.*, 2009, 2010). Here we assessed the broader role of GIV's GEF function on insulin-triggered signaling pathways that are known to have opposing effects on autophagy: the PI3K-Akt-mTOR pathway, which inhibits autophagy (Meijer and Codogno, 2004), and phospho-ERK1/2 in the Ras-Raf-MEK-ERK pathway, which promotes autophagy (Ogier-Denis *et al.*, 2000; Wang *et al.*, 2009). To assess the role of GIV's GEF function, we depleted endogenous GIV from HeLa–GIV-WT and HeLa–GIV-FA cells and analyzed these cells by immunoblotting for activation (phosphorylation) of protein substrates within the PI3K-mTOR (Akt, S6 kinase [S6K], and S6 ribosomal protein) or Ras-ERK pathways. On insulin stimulation, phosphorylation of Akt, S6K, and S6 ribosomal proteins was significantly higher in GIV-WT cells than in GIV-FA cells at 5–30 min (Figure 1, F and G), whereas ERK1/2 phosphorylation was down-regulated by 15–30 min in GIV-WT but enhanced and sustained for greater than 30 min in GIV-FA cells. Because GIV's ability to bind and/or activate $G\alpha_i$ (Garcia-Marcos *et al.*, 2009) is the key difference between GIV-WT and GIV-FA cells, our results indicate that activation of $G\alpha_i$ by GIV's GEF function is required for enhancement of the Akt-mTOR pathway and for down-regulation of the Ras-ERK1/2 pathway in response to insulin. We conclude that GIV's GEF function promotes insulin responsiveness in part by enhancing anti-autophagic signaling pathways.

GIV and AGS3 reversibly modulate $G\alpha_{i3}$ activity

Because GIV suppresses autophagy by activating $G\alpha_{i3}$ and AGS3 promotes autophagy by maintaining $G\alpha_i$ in an inactive state (Pattingre *et al.*, 2003), we reasoned that the anti-autophagic functions of GIV and the proautophagic AGS3 might be due to their ability to antagonize each other in modulating $G\alpha_{i3}$ activity. AGS3 locks $G\alpha_{i3}$ in an inactive state by blocking its ability to exchange nucleotides (De Vries *et al.*, 2000; Peterson *et al.*, 2000), whereas GIV activates $G\alpha_{i3}$ by accelerating its rate of nucleotide exchange (Garcia-Marcos *et al.*, 2009). We investigated whether GIV can activate $G\alpha_{i3}$ when $G\alpha_{i3}$ is in a complex with AGS3 by measuring the steady-state GTPase activity of the G protein (Garcia-Marcos *et al.*, 2009). We purified His-$G\alpha_{i3}$:GST-AGS3 complexes (4:1 stoichiometry; Figure 2A) and found that the GTPase activity of $G\alpha_{i3}$ in these complexes was reduced 15.3 ± 4.3% compared with $G\alpha_{i3}$ alone ($n = 3$, $p < 0.05$; unpublished data). The stoichiometry of these

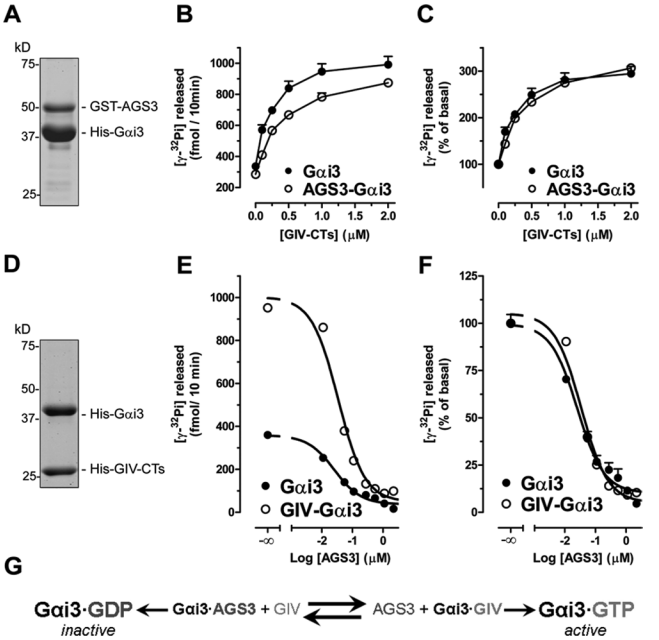

FIGURE 2: $G\alpha_{i3}$ activity is reversibly modulated by GIV (a GEF) and AGS3 (a GDI). (A) Preparation of $G\alpha_{i3}$–AGS3 complexes. His-$G\alpha_{i3}$:GST-AGS3 (465–650) complexes were purified (4:1 stoichiometry) by glutathione-agarose affinity chromatography. An aliquot of the purified complex was separated by SDS–PAGE and stained with Coomassie blue. (B, C) GIV efficiently promotes G protein activation in the $G\alpha_{i3}$–AGS3 complex. The steady-state GTPase activity of purified His-$G\alpha_{i3}$ (50 nM) alone (closed circles) or in complex with GST-AGS3 (open circles) was determined in the presence of the indicated amounts (0, 0.1, 0.25, 0.5, 1, and 2 μM) of purified His-GIV-CTs (aa 1660–1870, containing the GEF motif responsible for $G\alpha_i$ binding) by quantification of the amount of [γ-^{32}P]GTP (0.5 μM, ~50 cpm/fmol) hydrolyzed in 10 min. Data are expressed as fmol of radioactive phosphate (^{32}Pi) released (absolute GTPase activity, B). The same data were normalized to the GTPase activity in the absence of His-GIV-CTs and expressed as % of ^{32}Pi released (fold activation, C) by the G protein alone (closed circles) or in complex with GST-AGS3 (open circles) in the absence of His-GIV-CTs. Results are shown as mean ± SD of a representative experiment out of three performed in duplicate. (D) Preparation of $G\alpha_{i3}$:GIV-CT complexes. His-$G\alpha_{i3}$:His-GIV-CTs (aa 1660–1870) complexes were purified (1:1 stoichiometry) by gel filtration chromatography. An aliquot of the purified complex was separated by SDS–PAGE and stained with Coomassie blue. (E, F) AGS3 efficiently blocks G protein activation in the $G\alpha_{i3}$–GIV complex. The steady-state GTPase activity of purified His-$G\alpha_{i3}$ (50 nM) alone (closed circles) or in complex with His-GIV-CTs (open circles) was determined in the presence of the indicated amounts (0, 0.11, 0.055, 0.11, 0.275, 0.55, 1.1, and 2.2 μM) of purified His-AGS3 (aa 424–650) by quantification of the amount of [γ-^{32}P]GTP (0.5 μM, ~50 cpm/fmol) hydrolyzed in 10 min. Data are expressed as fmol radioactive phosphate (^{32}Pi) released (absolute GTPase activity, E). The same data were normalized to the GTPase activity in the absence of His-AGS3 and expressed as % of ^{32}Pi released (fold activation, F) by the G protein alone (closed circles) or in complex with His-GIV-CTs (open circles) in the absence of His-AGS3. Results are shown as mean ± SD of a representative experiment out of three performed in duplicate. (G) Schematic representation of the reversible regulation of $G\alpha_{i3}$ activity by AGS3 GDI and GIV GEF.

complexes and their G protein activity are consistent with previous reports (Tall and Gilman, 2005; Thomas *et al.*, 2008). Addition of His-GIV terminus (CTs) (aa 1660–1870, which contains GIV's GEF motif) increased the GTPase activity of His-$G\alpha_{i3}$:GST-AGS3

complexes and His-Gα_{i3} alone in a dose-dependent manner (Figure 2B) and with equal potency (up to approximately threefold in the presence of 2 μM His-GIV-CTs, the maximal concentration tested) (Figure 2C). These results demonstrate that GIV's GEF function can efficiently activate Gα_{i3} when the latter is complexed with the GDI AGS3.

Next we investigated whether AGS3 could similarly inhibit Gα_{i3} when the latter is in a complex with GIV and found indeed this is the case: The activity of Gα_{i3} in purified His-Gα_{i3}:His-GIV-CTs complexes (1:1 stoichiometry; Figure 2D) was increased approximately threefold compared with uncomplexed Gα_{i3} (Figure 2E), which is consistent with the maximal activation achieved by His-GIV-CTs in dose-response studies (Figure 2C) (Garcia-Marcos *et al.*, 2009, 2010). Addition of His-AGS3 inhibited the GTPase activity of both His-Gα_{i3} and His-Gα_{i3}:His-GIV-CTs in a dose-dependent manner (Figure 2E) and with equal potency (Figure 2F), virtually abolishing it in the presence of 2.2 μM His-AGS3, the maximum concentration tested. These results demonstrate that AGS3 can efficiently inhibit Gα_{i3} when the latter is complexed with its GEF, GIV.

Taken together these results indicate that the regulation of Gα_{i3} activity by AGS3 and GIV works as a reversible reaction that can proceed in either direction, that is, activation or inactivation, depending on the relative concentrations of AGS3 and GIV (see Figure 2G).

GIV and AGS3 compete for binding to Gα_{i3}

To investigate whether reversible modulation of Gα_{i3} activity by GIV and AGS3 depends on their intermolecular interactions, we took advantage of the available structural information. We compared the homology model (Figure 3A) of GIV's GEF motif bound to Gα_{i3}, which we previously validated (Garcia-Marcos *et al.*, 2009), with the crystal structure of Gα_{i1} bound to the G$\alpha_{i/o}$-Loco (GoLoco) motif of RGS14, which is homologous to the GoLoco motifs in AGS3 that are responsible for its GDI activity (Kimple *et al.*, 2002). Comparative analysis revealed that GIV's GEF and RGS14's GoLoco motifs have overlapping binding sites on Gα_i in that both dock onto the cleft formed between the switch II and the α3 helix of the G protein (Figure 3A), suggesting that AGS3 and GIV might compete for binding to Gα_{i3}. To test this possibility, we first determined whether increasing concentrations of His-GIV-CTs are capable of displacing His-Gα_{i3} from His-Gα_{i3}:GST-AGS3 complexes and found that this is the case: With

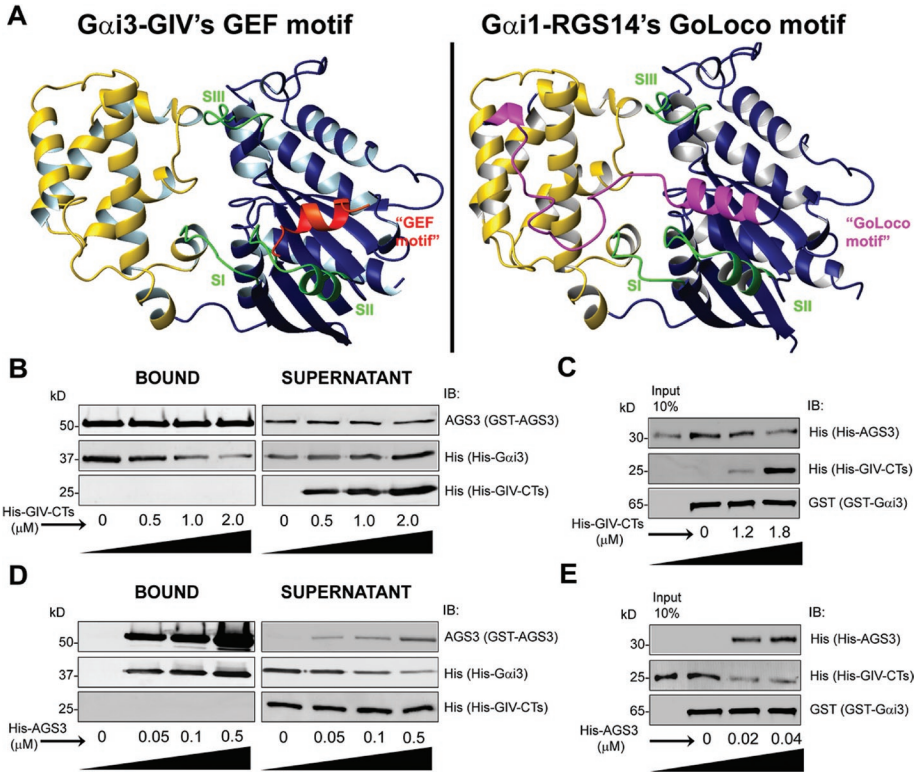

FIGURE 3: GIV-CTs and AGS3 compete for binding to Gα_{i3}. (A) GIV's GEF motif and RGS14's GoLoco motif have overlapping binding sites on Gα_i subunits. Left, a homology model of GIV's GEF motif (shown in red) bound to GDP–Gα_{i3} was generated as described previously (Garcia-Marcos *et al.*, 2009) using the structure of the synthetic peptide KB-752 bound to Gα_{i1} (PDB:1Y3A) as a template. Right, structural model of RGS14's GoLoco motif (shown in pink) bound to Gα_{i1} was generated using the coordinates of the published crystal structure (Kimple *et al.*, 2002). In both panels, the "ras-like" domain of Gα_{i3} is shown in blue, the "all-helical" domain in yellow, and the three "switch" regions (SI, SII, and SIII) in green. GIV's GEF and RGS14's GoLoco motifs dock onto the same cleft formed between the switch II and the α3 helix of the G protein. (B) GIV-CTs displaced Gα_{i3} from Gα_{i3}–AGS3 complexes. Purified His-Gα_{i3}:GST-AGS3 complexes were incubated with increasing amounts of His-GIV-CT (0, 0.5, 1, and 2 μM), and subsequently the GST–AGS3-bound complexes were immobilized on glutathione-agarose beads followed by centrifugation. GST–AGS3-bound proteins in the pellet were eluted with SDS–PAGE sample buffer. Bound proteins (left panel) and unbound proteins (right panel) were analyzed for His (His-Gα_{i3}, His-GIV-CTs) and AGS3 (GST-AGS3) by immunoblotting (IB). His-Gα_{i3} was simultaneously depleted from the GST–AGS3-bound fraction (left panel) and enriched in the supernatant (right panel). Note that under these experimental conditions binding of His-Gα_{i3}:GST-AGS3 complexes to glutathione-agarose beads is incomplete, as evidenced by its presence in the supernatant even in the absence of His-GIV-CTs (right panel, first lane). (C) GIV-CTs displaces AGS3 from Gα_{i3}–AGS3 complexes. GST–Gα_{i3} was incubated with His-AGS3 (0.1 μg) overnight at 4°C. The unbound His-AGS3 was washed, and the GST–Gα_{i3}-bound complexes were then incubated with increasing amounts His-GIV-CTs (0, 1.2, 1.8 μM). GST–Gα_{i3}-bound proteins were eluted with SDS–PAGE sample buffer and analyzed for His (His-GIV-CTs, His-AGS3) and Gα_{i3} (GST-Gα_{i3}) by IB. Increased His-GIV-CTs binding to GST-Gα_{i3} are accompanied by decreased His-AGS3 binding. (D) AGS3 sequesters Gα_{i3} from Gα_{i3}–GIV complexes. Purified His-Gα_{i3}:His-GIV-CTs complexes were incubated with increasing amounts of GST–AGS3 (0, 0.05, 0.1, and 0.5 μM), and the resulting GST–AGS3-bound complexes were immobilized on glutathione-agarose beads followed by centrifugation. GST–AGS3-bound proteins in the pellet were eluted with SDS–PAGE sample buffer. Bound proteins (left panel) and unbound proteins (right panel) were analyzed for His (His-Gα_{i3}, His-GIV-CTs) and AGS3 (GST-AGS3) by IB. His-Gα_{i3} was depleted from the supernatant (right panel) and concomitantly enriched in the GST–AGS3-bound complexes with increasing His-GIV-CTs concentration. (E) AGS3 displaces GIV from Gα_{i3}–GIV complexes. GST–Gα_{i3} was incubated with His-GIV-CTs (6 μg) overnight at 4°C. The unbound His-GIV-CTs were washed, and the GST–Gα_{i3}-bound complexes were incubated with increasing amounts His-AGS3 (0, 0.02, and 0.04 μM). GST–Gα_{i3}-bound proteins were eluted with SDS–PAGE sample buffer and analyzed for His (His-GIV-CTs, His-AGS3) and Gα_{i3} (GST–Gα_{i3}) by IB. Increased binding of His-AGS3 to GST–Gα_{i3} is accompanied by decreased His-GIV-CTs binding. AGS3 displaced GIV from Gα_{i3} at lower concentrations (D, E) than those required for GIV to displace AGS3 (B, C), which is consistent with the fact that AGS3 has four Gα_i binding sites with Kd ≈ 30–100 nM (Adhikari and Sprang, 2003), and GIV has only one binding site with Kd ≈ 300 nM (unpublished data).

increasing concentrations of His-GIV-CTs, the amount of His-Gα_{i3} bound to immobilized GST-AGS3 decreased with a concomitant release of His-Gα_{i3} into the supernatant (Figure 3B), suggesting that GIV competes with AGS3 for binding to Gα_{i3} and can displace AGS3 from Gα_{i3}. We confirmed this finding using a complementary approach in which His-AGS3 was prebound to immobilized GST-Gα_{i3} and subsequently incubated with increasing amounts of His-GIV-CTs. GIV displaced AGS3 from Gα_{i3}, as evident from the decreased amount of His-AGS3 bound to immobilized GST-Gα_{i3} and the concomitant increase in His-GIV-CTs binding (Figure 3C). Finally, using GST-Gα_{i3} and Cos7 cell lysate or rat brain as the source of full-length AGS3, we confirmed that His-GIV-CTs is also capable of competing with and displacing full-length AGS3 from Gα_{i3} (unpublished data).

To investigate whether AGS3 competes with GIV for Gα_{i3} binding, we carried out similar assays in which we incubated His-Gα_{i3}:His-GIV-CTs complexes (Figure 3D) with increasing concentrations of GST-AGS3; the latter was subsequently immobilized on glutathione-agarose beads and analyzed for bound Gα_{i3}. His-Gα_{i3} binding to GST-AGS3 was accompanied by decreased Gα_{i3} binding to GIV-CT from the His-Gα_{i3}:His-GIV-CT complexes in the supernatant (Figure 3D), suggesting that AGS3 sequesters Gα_{i3} from His-Gα_{i3}:His-GIV-CT complexes by competing with and displacing GIV. We confirmed this finding using a complementary approach in which His-AGS3 displaced His-GIV-CTs prebound to immobilized GST-Gα_{i3} (Figure 3E). Furthermore, analysis of Gα_{i3}-bound complexes immunoprecipitated from Cos7 cells expressing Gα_{i3}-FLAG revealed that expression of HA-AGS3 virtually abolished binding of GIV to Gα_{i3} and confirmed that full-length AGS3 competes with and displaces full-length GIV in vivo (unpublished data). In addition, using localization of GFP-LC3 to assess autophagic activity (as in Figure 1A), we confirmed prior observations by others (Pattingre *et al.*, 2003) that AGS3 promotes autophagic activity in serum-starved cells and inhibits the anti-autophagic action of growth factors (unpublished data). We conclude that the reversible modulation of Gα_{i3} activity by AGS3 and GIV (Figure 2) during promotion or inhibition of autophagy, respectively, is a consequence of their competition for binding to the same site in Gα_{i3}.

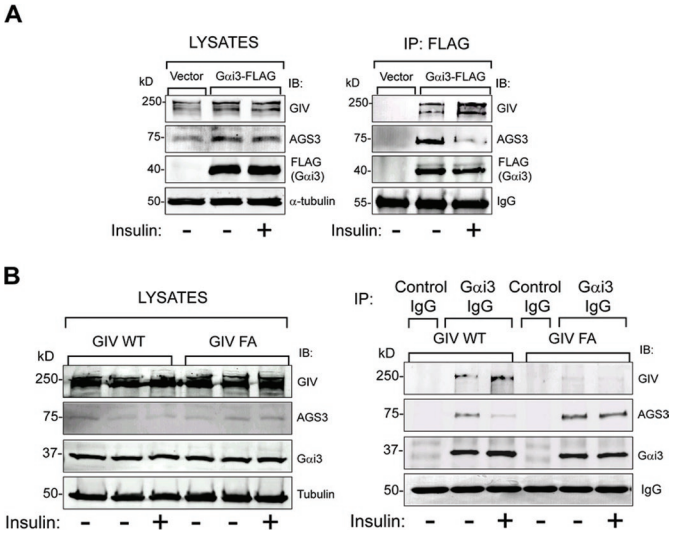

FIGURE 4: GIV's GEF motif is required for insulin to trigger a shift in Gα_{i3} binding from AGS3 to GIV. (A) Gα_{i3} coimmunoprecipitates with AGS3 in serum-starved cells and with GIV when cells are insulin stimulated. Cos7 cells transiently transfected with FLAG-tagged Gα_{i3} (Gα_{i3}-FLAG) or vector control were serum starved (–) and stimulated with 100 nM insulin (+) for 15 min before lysis. Equal aliquots of cell lysates (left panel) were incubated with anti-FLAG mAb. Immunoprecipitated complexes (right panel) were analyzed for GIV, AGS3, and FLAG (Gα_{i3}) by immunoblotting (IB). In serum-starved cells (–), Gα_{i3}-bound immune complexes are enriched in AGS3, whereas after insulin treatment (+) these immune complexes are depleted of AGS3 and enriched in GIV. Identical observations were made after EGF treatment (Supplemental Figure S4). (B) Changes in the abundance of Gα_i–AGS3 complexes in response to insulin require an intact GEF motif in GIV. Immunoprecipitation was carried out on lysates of serum-starved and insulin-stimulated control, GIV-WT, and GIV-FA cells with anti-Gα_{i3} IgG, and the immune complexes were analyzed for Gα_{i3}, AGS3, and GIV by IB. In GIV-WT cells, the amount of Gα_{i3}-bound GIV increased and the amount of Gα_{i3}-bound AGS3 decreased upon insulin treatment. In GIV-FA cells (GEF-deficient mutant), GIV does not coimmunoprecipitate with Gα_{i3}, and the extent of Gα_{i3}-bound AGS3 remains unaltered after insulin treatment.

Insulin stimulation promotes binding of GIV to Gα_{i3} during recovery from starvation-induced autophagy

Next we investigated whether growth factors influence the competitive binding of GIV and AGS3 to Gα_{i3} in vivo. When we immunoprecipitated Gα_{i3} from Cos7 cells expressing Gα_{i3}-FLAG and immunoblotted for AGS3 and GIV, we found that AGS3 interacted with Gα_{i3} preferentially upon starvation, and this interaction was reduced by ~75–80% upon insulin stimulation (Figure 4A). In contrast, GIV displayed an approximately twofold increase in binding to Gα_{i3} compared with the starved state. Identical results were obtained when the cells were stimulated with EGF (Supplemental Figure S4), indicating that the pattern is common to several growth factors. These results demonstrate that starvation favors formation of AGS3–Gα_{i3} complexes, whereas growth factors favor formation of GIV–Gα_{i3} complexes and dissociation of AGS3–Gα_{i3} complexes. We conclude that AGS3–Gα_{i3} and GIV–Gα_{i3} complexes exist in equilibrium in living cells and that growth factor stimulation shifts the equilibrium toward activation of Gα_{i3} by GIV. We anticipated that this shift might require the presence of a functional GEF motif in GIV and found that this is indeed the case. Comparison of the endogenous Gα_{i3}-bound complexes in starved and insulin-stimulated GIV-WT and GIV-FA cells revealed that the insulin-dependent shift from AGS3–Gα_{i3} to GIV–Gα_{i3} complexes occurred exclusively in GIV-WT cells (Figure 4B). The ability of insulin to increase GIV–Gα_{i3} complexes and reduce AGS3–Gα_{i3} complexes in GIV-WT but not in GIV-FA cells correlates with the responsiveness of these cells to insulin (Figure 1, A and B), suggesting that GIV's ability to antagonize AGS3 (Figures 2 and 3) is required for the anti-autophagic action of insulin. We conclude that GIV's GEF function facilitates the anti-autophagic action of insulin in part by shifting the equilibrium from AGS3–Gα_{i3} toward GIV–Gα_{i3} and triggering activation of Gα_{i3}.

AGS3 localizes to LC3-positive membranes and directly interacts with LC3

Gα_{i3} has been recently reported to localize to LC3-positive vesicles in starved cells, from which it presumably exerts its function in promoting autophagy (Gohla *et al.*, 2007). We asked whether AGS3, which is known to bind and inactivate Gα_{i3} during autophagy, also localizes to LC3-positive vesicles and found that this is the case. Using prepermeabilization and an affinity-purified rabbit polyclonal antibody characterized previously (De Vries *et al.*, 2000; Pattingre *et al.*, 2003), we found that a pool of AGS3 colocalized with GFP-LC3–positive vesicles in HeLa cells (Figure 5A). Next we investigated whether AGS3 interacts with LC3 when GFP-LC3 and HA-AGS3 are coexpressed in Cos7 cells. AGS3 and LC3 were found in the same immune complexes after immunoprecipitation with either GFP

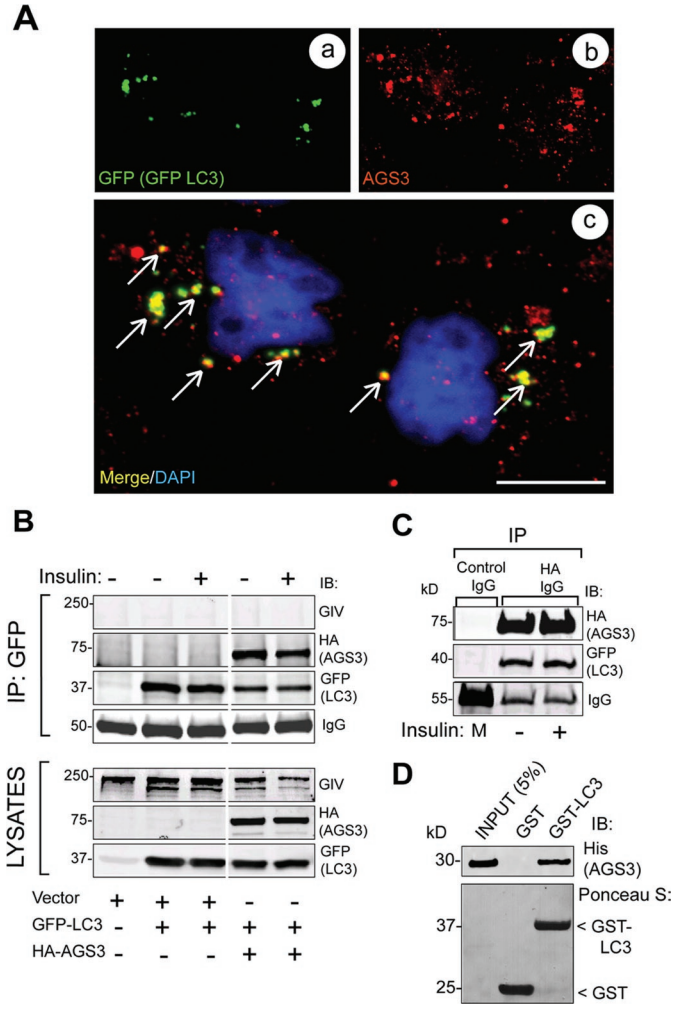

FIGURE 5: AGS3 localizes to autophagosomes and interacts with the autophagy effector LC3. (A) GFP-LC3 and endogenous AGS3 partially colocalize on vesicular structures in serum-starved cells. HeLa cells expressing GFP-LC3 were serum starved (0.2% FBS) in the presence of leupeptin and pepstatin. Cells were permeabilized with 0.05% saponin, fixed, stained for LC3 (GFP, green, a) and for AGS3 (red, b), and analyzed by confocal microscopy. The merged panel (c) shows that AGS3 colocalizes with GFP-LC3 (yellow pixels, arrows) on some of the punctate autophagic structures. Bar = 10 μM. (B) AGS3 coimmunoprecipitates with GFP-LC3 in vivo. Cos7 cells transiently cotransfected with GFP-LC3, and either AGS3-HA or vector control were serum starved as in (A) and then treated with insulin before lysis. Equal aliquots of cell lysates (bottom panels) were treated with GFP mAb, and immuno-precipitated complexes (top panels) were analyzed for AGS3 (HA), LC3 (GFP), and GIV by immunoblotting (IB). AGS3 and LC3 interact both in serum-starved and insulin-stimulated cells. (C) LC3 coimmunoprecipitates with AGS3-HA. Lysates of Cos7 cells coexpressing GFP-LC3 and AGS3-HA (as above) were treated with HA mAb, and a 1:1 mix (M) of the two lysates was treated with mouse preimmune IgG. Immunoprecipitated complexes were analyzed for AGS3 (HA) and LC3 (GFP) by IB. AGS3 and LC3 coimmunoprecipitate in both serum-starved and insulin-stimulated cells. (D) His-AGS3 (aa 424–650) directly interacts with GST-LC3. Equal aliquots (15 μg) of GST or GST-LC3 were used in pull-down assays with 3 μg His-AGS3. Bound proteins were visualized by IB for His-AGS3. AGS3 binds GST-LC3 but not the GST control.

(Figure 5B) or HA (Figure 5C) IgG and did so regardless of whether or not cells were stimulated with insulin. Also, GST-LC3 bound purified His-AGS3 (Figure 5D), indicating that the LC3–AGS3 interaction is direct. These results demonstrate that AGS3 localizes to LC3-rich autophagosomal vesicles and interacts directly and constitutively with LC3, an autophagic effector and autophagosomal resident protein.

$G\alpha_{i3}$ is recruited to LC3 by AGS3 and is released by GIV's GEF function

To investigate whether $G\alpha_{i3}$ is present in the same complexes as LC3 and AGS3 in vivo, we immunoprecipitated LC3 from HeLa cells expressing GFP-LC3 and immunoblotted the immune complexes for AGS3 and $G\alpha_{i3}$. To maximize the detection of small amounts of endogenous proteins, cells were either maintained in 10% FBS or starved in the presence of lysosomal protease inhibitors (leupeptin and pepstatin) to stop protein degradation and promote the accumulation of complexes on mature autophagolysosomes (Gohla *et al.*, 2007). Endogenous $G\alpha_{i3}$ coimmunoprecipitated with LC3 exclusively in starved cells, whereas endogenous AGS3 interacted with LC3 irrespective of the nutrient status (Figure 6A), indicating that $G\alpha_{i3}$, AGS3, and LC3 can form part of the same molecular complex in vivo only after serum starvation. Using purified proteins in pull-down assays, we found that $G\alpha_{i3}$ binds LC3 exclusively in the presence of AGS3 (Figure 6B, "bound" panels, lanes 1–4). Taken together these results demonstrate that AGS3 interacts constitutively with LC3, whereas the interaction between $G\alpha_{i3}$ and LC3 observed in starved cells (Figure 6A) is indirect and is via AGS3.

On the basis of our finding that GIV disrupts $G\alpha_{i3}$–AGS3 interaction via its GEF motif, we reasoned that GIV might similarly dissociate and release $G\alpha_{i3}$ from GST-LC3:His-AGS3:His-$G\alpha_{i3}$ complexes. We found that such is the case because His-GIV-CTs' wild type, but not GEF-deficient GIV-FA mutant, displaced $G\alpha_{i3}$ from GST-LC3:His-AGS3:His-$G\alpha_{i3}$ complexes in vitro (Figure 6B, lanes 5–8). We conclude that GIV and AGS3 have opposite effects on the association of $G\alpha_{i3}$ with LC3; that is, AGS3 promotes formation of $G\alpha_{i3}$–LC3 complexes whereas GIV releases $G\alpha_{i3}$ from these complexes, suggesting that association of $G\alpha_{i3}$ with LC3 and thereby with autophagosomes is regulated by AGS3 and GIV.

GIV's GEF function is required to release $G\alpha_{i3}$ from LC3-positive membranes upon insulin stimulation

$G\alpha_{i3}$ has been localized to LC3-positive membranes, possibly autophagolysosomes, by immunofluorescence and by cell fractionation during starvation-induced autophagy (Gohla *et al.*, 2007), and we found that $G\alpha_{i3}$ associates with LC3 exclusively upon nutrient starvation (Figure 6A). To investigate whether GIV's GEF function regulates association of $G\alpha_{i3}$ with LC3-positive membranes, we set up a previously validated biochemical assay (Gao *et al.*, 2010) in which we immunoisolated GFP-LC3–positive autophagosomes from starved HeLa cells and immunoblotted for $G\alpha_{i3}$ (Figure 6C). Our GFP-LC3 immunoisolates were devoid of contaminants from other organelles such as Golgi, endosomes, lysosomes, or the nucleus. However, we found $G\alpha_{i3}$ in these immunoisolates, thus supporting previous observations by several groups that $G\alpha_{i3}$ localizes to different autophagosomal structures (Garin *et al.*, 2001; Gotthardt *et al.*, 2006; Gohla *et al.*, 2007; Stuart *et al.*, 2007; Gao *et al.*, 2010). Using this assay we compared the levels of $G\alpha_{i3}$ associated with GFP-LC3–immunoisolated membranes in starved or insulin-stimulated GIV-WT, GIV-FA, and control HeLa cell lines. $G\alpha_{i3}$ was detected in GFP-LC3 immunoisolates from all starved cells lines before insulin stimulation (Figure 6D). After 5 min insulin stimulation, $G\alpha_{i3}$ was not detected in immunoisolated GFP-LC3–positive membranes in control and GIV-WT cells, whereas in GIV-FA cells there was no change after insulin stimulation. These findings suggest that activation of

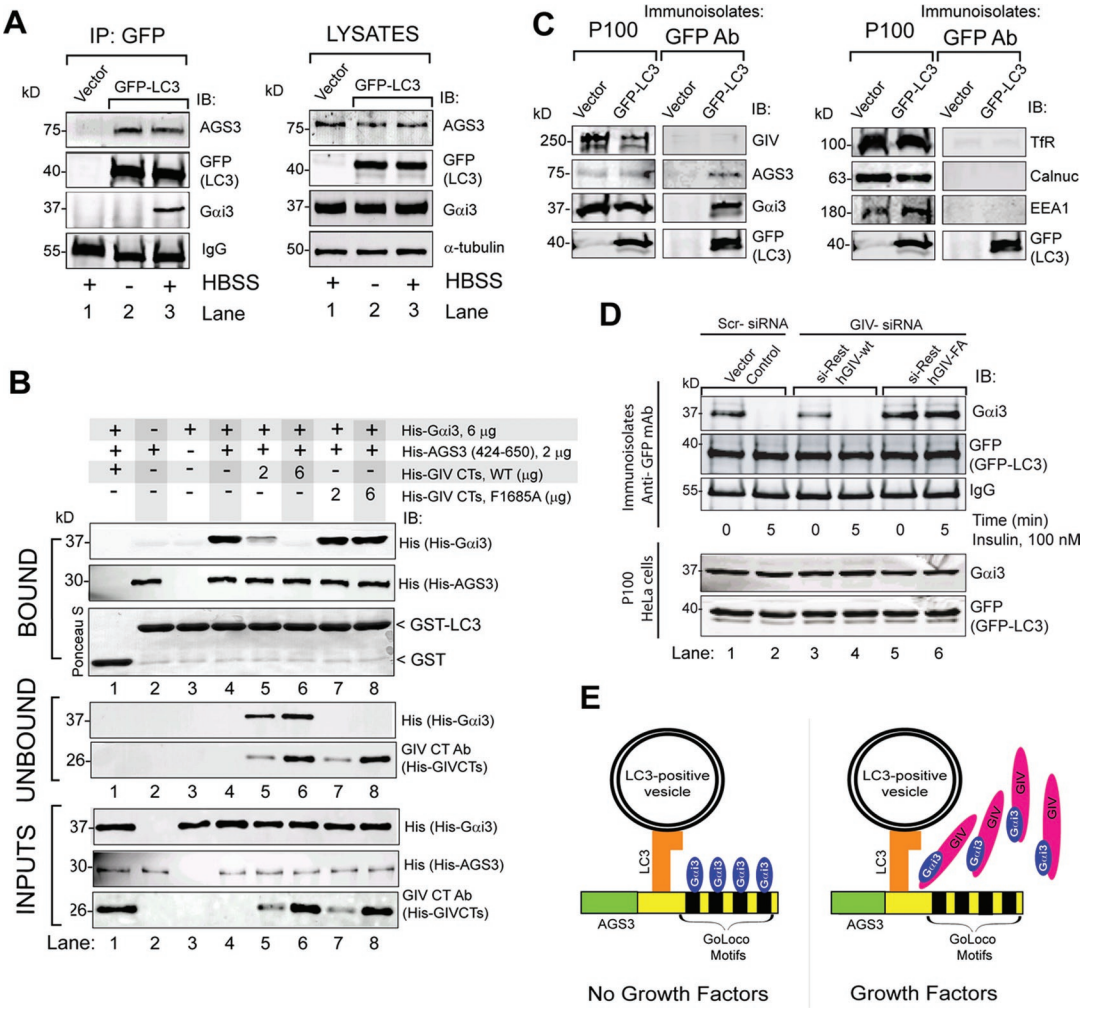

FIGURE 6: AGS3 links $G\alpha_{i3}$ to LC3 by forming a ternary ($G\alpha_{i3}$–AGS3–LC3) complex, and GIV's GEF motif is required for the release of $G\alpha_{i3}$ from this complex. (A) Endogenous AGS3 and $G\alpha_{i3}$ coimmunoprecipitate with GFP-LC3. HeLa cells expressing GFP-LC3 or vector control were maintained in either 10% FBS (−) or Hank's balanced salt solution (HBSS) media (+) in the presence of leupeptin and pepstatin for 12 h before lysis. Immunoprecipitation was carried out on equal aliquots of cell lysates (right panel) using anti-GFP IgG, and the bound immune complexes (lanes 1–3) were analyzed for LC3 (GFP-LC3), $G\alpha_{i3}$, and AGS3 by immunoblotting (IB, left panel). AGS3 is present in LC3-bound complexes under both 10% serum (−) and HBSS-starved (+) conditions (lanes 2 and 3), whereas $G\alpha_{i3}$ is present exclusively upon starvation (lane 3). Neither AGS3 nor $G\alpha_{i3}$ were detected in GFP immunoprecipitates from cells transfected with vector control (lane 1). (B) His-$G\alpha_{i3}$ binds GST-LC3 in the presence of His-AGS3 and can be displaced by His-GIV-CTs WT, but not by His-GIV-CTs FA. Equal aliquots of GST (lane 1) or GST-LC3 (15 μg, lanes 2–8) were incubated with either His-AGS3 alone (lane 2), His-$G\alpha_{i3}$ alone (lane 3), or both proteins simultaneously (lanes 1 and 4–8) for 8–12 h at 4°C. After removing the unbound excess, GST–LC3-bound complexes were subjected to a second binding assay with increasing amounts (2 and 6 μg) of either WT His-GIV-CTs (lanes 5 and 6) or FA-mutant (lanes 7 and 8) (see bottom panel, "inputs"). GST–LC3-bound proteins were eluted with sample buffer and "bound" and "unbound" proteins were analyzed for $G\alpha_{i3}$ (His-$G\alpha_{i3}$), AGS3 (His-AGS3), and GIV (His-GIV-CTs). AGS3 directly binds LC3 (top panels, lane 2), but $G\alpha_{i3}$ binds LC3 exclusively in the presence of AGS3 (top panels, compare lanes 3 and 4). His-GIV-CTs WT decreased the amount of His-$G\alpha_{i3}$ bound to GST-LC3 (top panels, lanes 5 and 6) and concomitantly increased the amount of His-$G\alpha_{i3}$ released into the supernatants (middle panel, lanes 5 and 6). In the case of mutant His-GIV-CTs FA, the amount of His-$G\alpha_{i3}$ bound to GST-LC3 did not change (top panels, lanes 7 and 8). (C) Immunoisolation of GFP-LC3–positive vesicles. HeLa cells expressing GFP-LC3 or vector control were serum starved in the presence of leupeptin and pepstatin, homogenized, and processed for subcellular fractionation (see *Materials and Methods*). The crude membrane fraction (P100) was resuspended in homogenization buffer and incubated with anti-GFP IgG (mAb) and protein G beads. Equal aliquots of the P100 or immunoisolated LC3-positive membranes (immunoisolates: GFP antibody) were immunoblotted for GIV, AGS3, $G\alpha_{i3}$, GFP-LC3 (left panels), and various organelle markers: transferrin receptor (Tfr, endosomes), EEA1 (early endosomes), calnuc (ER-Golgi), and GFP-LC3 (autophagosomes) (right panels). GFP-LC3, AGS3, and $G\alpha_{i3}$ were detected in the GFP immunoisolates whereas GIV, Tfr, EEA1, and calnuc were not. Additionally, βCOP, cathepsin D, and lamin A, markers of ER-Golgi, lysosomes, and nuclear envelope, respectively, were also undetectable (unpublished data), indicating that LC3-positive membrane isolates were free of significant contaminants. (D) Upon insulin stimulation, $G\alpha_{i3}$ is depleted from immunoisolated LC3-positive vesicles in GIV-WT but not GIV-FA cells. Control, GIV-WT, and GIV-FA HeLa cells were treated with scrambled (Scr) or GIV siRNA, followed by transient transfection with GFP-LC3 as in Figure 1B. Cells were

$G\alpha_{i3}$ by GIV's GEF function is required for release of $G\alpha_{i3}$ from LC3-positive membranes after insulin stimulation. On the basis of our findings, we propose (Figure 6E) that in the absence of growth factors inactive $G\alpha_{i3}$ is recruited to LC3-positive membranes via its interaction with GoLoco motifs on AGS3, which directly binds LC3 on phagosome membranes. In the presence of growth factors, activation of $G\alpha_{i3}$ by GIV's disrupts its association AGS3–LC3 complexes, provoking release of $G\alpha_{i3}$ from LC3-positive membranes. Taken together with our finding that GIV's GEF function is required for enhancement of anti-autophagic growth factor signals (Figure 1), we propose a working model in which GIV inhibits autophagy by coordinately promoting $G\alpha_{i3}$ release from $G\alpha_{i3}$–AGS3–LC3 complexes on membranes and enhancing anti-autophagic growth factor signaling (see Figure 7A legend).

Analysis of protein–protein interaction map

To better understand the molecular links between the autophagic machinery, growth factor receptors, G proteins, and GIV, we generated a protein–protein interaction map using the interologous interaction database (Brown and Jurisica, 2005; Brown *et al.*, 2009) and STRING (von Mering *et al.*, 2005), a functional interaction database. It shows that the shortest link between G protein and the autophagic machinery is via AGS3 and that AGS3 links inactive Gi to LC3. On the other hand, GIV links a variety of growth factor receptors and the anti-autophagic PI3K-mTOR pathway via active $G\alpha_i$. The entire web of pro- and anti-autophagic pathways summarized in the network is on average only two protein–protein interactions away from the G protein $G\alpha_{i3}$, which serves as the pivot of a seesaw-like balance flanked by AGS3 and GIV. This is in keeping with our findings and proposed model that AGS3 and GIV antagonistically balance G protein activity and thereby maintain the delicate equilibrium of autophagy. In support of their antagonistic roles in regulating autophagy, AGS3 has no direct link to anti-autophagic growth factor signals (Figure 7B, red) and GIV has no direct link to the proautophagic machinery (Figure 7B, green). In addition to the autophagy-related interactions, a number of direct and indirect interactions occur between G proteins or their modulators and proteins that mediate asymmetric cell division (Figure 7B, yellow) or regulate apoptosis (Figure 7B, blue). Such signaling interactions imply coordination between autophagy, apoptosis, and cell division, all of which are known to involve nutrient sensing, G proteins, and growth factor receptors (Willard *et al.*, 2004; Yanamadala *et al.*, 2009).

DISCUSSION

GIV regulates autophagy by balancing G protein activity and growth factor signals

In this work we describe GIV, a nonreceptor GEF for $G\alpha_{i3}$ (Garcia-Marcos *et al.*, 2009), as a novel regulator of autophagy and provide mechanistic insights into how the roles of G protein activity and growth factor signaling are intertwined in regulation of autophagy. We found that HeLa–GIV-WT cells expressing GIV with a functional GEF motif show the expected increase in autophagy when starved and inhibition of autophagy when maintained in serum or when stimulated with insulin. By contrast, HeLa–GIV-FA cells expressing a GEF-deficient mutant of GIV that cannot activate $G\alpha_{i3}$ demonstrate high levels of autophagy not only when starved but also when grown in the presence of serum or after insulin stimulation. Because GIV-WT and GIV-FA cells differ by a single point mutation that selectively and specifically disrupts GIV's GEF activity (Garcia-Marcos *et al.*, 2009), we conclude that GIV inhibits autophagy in the presence of serum and orchestrates cellular recovery from autophagy by activating $G\alpha_i$ upon insulin stimulation.

We show that the striking differences in the levels of autophagy and insulin responsiveness between GIV-WT and GIV-FA cells are also accompanied by a contrasting set of signaling programs. Insulin-responsive GIV-WT cells preferentially enhance the anti-autophagic PI3K→Akt→mTOR pathway and inhibit the proautophagic Ras→Raf→MEKK→ERK1/2 signals, whereas insulin-resistant GIV-FA cells do the opposite. This indicates that GIV's GEF domain, which activates $G\alpha_i$, is crucial for the selective activation of the class 1 PI3K-mTOR pathway and suppression of the Ras-Raf-MEKK-ERK pathway, thereby creating a divergence in PI3K and ERK signals downstream of the insulin receptor. We recently reported that identical PI3K/Akt- versus ERK-divergent signaling is also observed when GIV-WT and GIV-FA cells are stimulated with EGF and showed that GIV's GEF function directly links $G\alpha_i$ activity to ligand-activated EGFR at the PM and thereby affects receptor autophosphorylation, adaptor recruitment, endocytic trafficking, and degradation (Ghosh *et al.*, 2010). It will be interest to determine whether GIV refines insulin receptor signals via similar mechanisms that involve G protein pathways. Consistent with this possibility, $G\alpha_i$ activation was implicated by others (Cao *et al.*, 2009) as a prerequisite for enhancement of mTOR signals by growth factors. Our findings identify GIV's GEF motif as the missing link between growth factor receptors and G protein–dependent mTOR signals.

We conclude that GIV regulates the cellular response to growth factors during autophagy via modulation of $G\alpha_i$ activity. Poised at the crossroads of G protein and growth factor signaling pathways (Ghosh *et al.*, 2010), GIV increases insulin responsiveness by activating $G\alpha_i$ and thereby coordinates cellular recovery from autophagy.

GIV's GEF function antagonizes pro-autophagic G protein signaling via AGS3, a GDI

Our finding that G protein activity is reversibly regulated by the antagonistic action of GIV (a GEF that activates Gi) and AGS3 (a GDI

serum starved and stimulated with insulin and homogenized, and equal aliquots of P100 fractions (100,000 × *g* pellets) (bottom panel) were incubated with GFP mAb for immunoisolation of GFP-LC3–positive membranes as in Figure 6C. Immunoisolates were analyzed for the presence of LC3 (GFP), $G\alpha_{i3}$, AGS3, and GIV by IB. $G\alpha_{i3}$ was detected in LC3-positive immunoisolates in all cell lines when serum starved (lanes 1, 3, and 5). Upon insulin treatment, $G\alpha_{i3}$ was undetectable in controls (lane 2) and GIV-WT cells (lane 4) but present in GIV-FA cells (lane 6). (E) Schematic representation of the interplay between $G\alpha_{i3}$, its modulators GIV and AGS3, and the autophagic effector LC3. In the absence of growth factors (left), AGS3 localizes to LC3-positive membranes by virtue of its direct, constitutive interaction within LC3. AGS3 recruits $G\alpha_{i3}$ to these LC3-positive membranes on which $G\alpha_{i3}$–AGS3–LC3 ternary complexes are assembled. On insulin stimulation (right), GIV binds $G\alpha_{i3}$ and releases it from the $G\alpha_{i3}$–AGS3–LC3 ternary complex assembled on membranes. This phenomenon is associated with inhibition of autophagosome formation and recovery from autophagy.

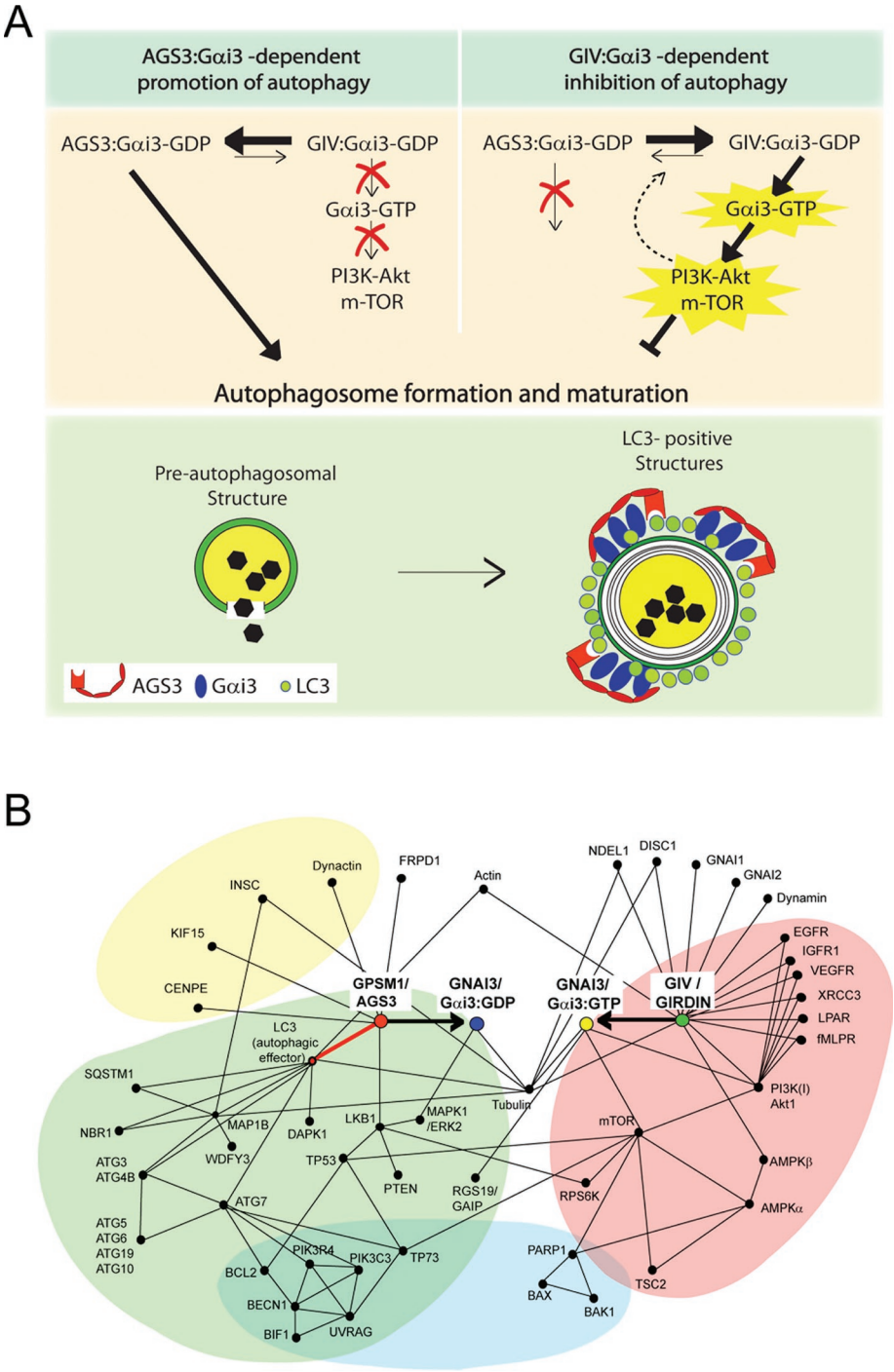

FIGURE 7: Proposed working model and protein–protein interaction map. (A) Working model. In the absence of growth factors (top left), $G\alpha_{i3}$ preferentially interacts with AGS3, its GDI, which maintains it inactive ($G\alpha_{i3}$–GDP). The $G\alpha_{i3}$–AGS3 complex localizes to LC3-positive structures via a direct interaction between AGS3 and LC3, thereby promoting autophagy (i.e., maturation of preautophagosomal structures into mature LC3-positive structures; green panel, bottom). In the presence of growth factors (top panel, right), $G\alpha_{i3}$ is activated ($G\alpha_{i3}$–GTP) by GIV, its GEF, which 1) enhances the anti-autophagic class I PI3K-Akt-mTOR signaling pathway at the PM and 2) releases active $G\alpha_{i3}$ from $G\alpha_{i3}$–AGS3–LC3 complexes assembled on membranes, thereby directly inhibiting autophagosome formation and maturation. It is possible that signaling programs modulated by GIV's GEF function at the PM also influence the equilibrium between $G\alpha_{i3}$–AGS3 and $G\alpha_{i3}$–GIV as a regulatory feedback loop (interrupted arrow). Further studies will be required to pinpoint the specific LC3-positive compartment where $G\alpha_{i3}$ localizes and the precise role of this G protein in regulating autophagosome maturation. (B) Proposed protein–protein interaction map for $G\alpha_{i3}$, GIV, and AGS3 showing the shortest functional links that integrate pro- or anti-autophagic signaling by growth factors and G protein pathways in balancing the process (initiation and reversal) of autophagy. Functional interactions between $G\alpha_{i3}$ and its modulators analyzed in this (GIV and AGS3) and other studies (RGS19/GAIP; Ogier-Denis *et al.*, 1997) in the context of autophagy are shown. These are based on interactions listed in the I2D (Brown and Jurisica, 2005; Brown *et al.*, 2009), STRING (http://string-db.org/), and MitoCheck (www.mitocheck.org) databases and validated in the literature. For simplicity, this interaction map includes only the experimentally validated functional interactions that are relevant to G protein and growth factor signaling during autophagy. The proteins of the autophagic pathway (green) are linked to $G\alpha_{i3}$ by a direct interaction (identified in this work and highlighted with a bold red line) between the GDI AGS3 (GPSM1) and LC3 (ATG8). The proteins of the anti-autophagic growth factor/nutrients (growth factor receptors, G protein–coupled receptors) and mTOR signaling pathways (red) are linked to G protein signaling via GIV (Girdin), the GEF that directly interacts with and activates $G\alpha_{i3}$ (resulting in $G\alpha_{i3}$–GTP). The protein network also reveals that processes such as apoptosis (blue) and asymmetric cell division (yellow) are likely to be influenced by modulation of G protein activity by either this or other such pairs of GDI(s) and GEF(s).

that inhibits Gi) provides a novel paradigm in the field of heterotrimeric G protein signaling. The canonical view of the G protein activation cycle depicts a unidirectional process in which G protein–coupled receptors (GPCRs; canonical GEFs) act on the heterotrimeric complex formed by Gα and Gβγ subunits (canonical GDI) (Gilman, 1987), with the unidirectionality of this process ensured by the fact that activation of Gα subunits by GPCRs cannot be antagonized by Gβγ. Recent work (Thomas *et al.*, 2008) on the nonreceptor GEF Ric-8A and the noncanonical GDI AGS3 also depicts a unidirectional process, that is, activation of Gα–AGS3 complexes by Ric-8A that cannot be antagonized by AGS3. We demonstrate here that regulation of $G\alpha_{i3}$ activity by GIV and AGS3 does not conform to the existing unidirectional paradigm—GIV can activate $G\alpha_i$–AGS3 complexes and, conversely, AGS3 can inhibit the activation of $G\alpha_i$–GIV complexes. Thus regulation of $G\alpha_{i3}$ activity by GIV and AGS3 is a bidirectional process and, as such, defines a novel paradigm in heterotrimeric G protein signaling.

We further provide the structural basis for such bidirectional signaling by demonstrating that GIV and AGS3 compete for binding to an overlapping site on $G\alpha_{i3}$. Of note, the structural features of AGS3

responsible for its GDI activity are highly conserved in other GoLoco motif–containing proteins (Willard *et al.*, 2004), rendering it likely that the molecular interplay between GIV and AGS3 in regulating G protein activity shown in this work applies to other GoLoco motif–containing GDIs. The biological relevance of such molecular interplay with GIV in other physiological processes in which GoLoco motif–containing proteins have been previously implicated (e.g., cell division) (Willard *et al.*, 2004) remains to be investigated.

Our results provide evidence that reversible regulation of $G\alpha_{i3}$ by GIV and AGS3 can occur in vivo in response to growth factors and that this phenomenon is regulated by GIV's GEF function. $G\alpha_{i3}$ preferentially interacts with its inhibitor, AGS3, in starved cells, whereas upon growth factor stimulation $G\alpha_{i3}$ preferentially interacts with its activator, GIV, thereby increasing the total G protein activity in vivo. This shift from AGS3–Gi to GIV–Gi complexes occurred exclusively in the presence of a functional GEF motif in GIV, indicating that the competitive binding of GEF and GDI to $G\alpha_i$ seen in vitro also occurs in vivo. The yin-yang effect of GIV and AGS3 on $G\alpha_{i3}$ described herein correlates with their respective roles in reversibly inhibiting and promoting autophagy and provides a physiological explanation for prior observations showing that constitutively active mutants of $G\alpha_{i3}$ inhibit whereas inactive mutants promote autophagy (Ogier-Denis *et al.*, 1996, 1997). The precise molecular mechanisms that govern growth factor–stimulated shifts in $G\alpha_i$-bound complexes from GDI to GEF in vivo remain unknown. We speculate that signaling programs (i.e., PI3K-Akt vs. ERK) that are initiated by growth factor receptors could trigger posttranslational modifications such as phosphorylation and/or altered localization of $G\alpha_{i3}$, AGS3, or GIV and thereby shift the composition of $G\alpha_{i3}$-bound complexes. Interestingly, these signaling programs are also modulated by GIV's GEF function (Figure 1, F and G), and it is possible that loops of feedback regulation exist (Figure 7A).

Regulation of $G\alpha_{i3}$ localization to LC3-positive membranes

Here we propose a model for the regulation of $G\alpha_{i3}$ localization to LC3-positive membranes by growth factors. Previous work (Gohla *et al.*, 2007) showed that upon serum starvation inactive $G\alpha_{i3}$ localizes to LC3-positive vesicular structures, probably autophagolysosomes; promotes autophagy; and is rapidly redistributed after insulin stimulation, coincident with recovery from autophagy. However, the basis for this dynamic localization has been poorly understood. We show that in the absence of growth factors $G\alpha_{i3}$ is found in LC3-positive membranes and exists in a complex with AGS3 and the autophagic effector LC3. Within these complexes AGS3 directly binds to LC3 and serves as the molecular bridge that recruits $G\alpha_{i3}$ to LC3-positive autophagosomal membranes during autophagy. After insulin stimulation $G\alpha_{i3}$ is released from immunoisolated LC3-positive membranes only when GIV's GEF motif is intact, consistent with the ability of GIV's GEF function to activate and release $G\alpha_{i3}$ from AGS3–LC3 complexes in vitro. Our results using the immunoisolation approach not only recapitulate prior observations made by immunofluorescence (Gohla *et al.*, 2007) but also provide the molecular basis for the dynamic cycling of $G\alpha_{i3}$ on and off autophagosomal membranes.

The precise LC3-positive compartment on which $G\alpha_{i3}$ localizes and the molecular mechanism by which $G\alpha_{i3}$ promotes autophagy are unclear. While Ghola and colleagues (2007) reported findings consistent with the presence of $G\alpha_{i3}$ on autophagolysosomes, a late autophagosomal compartment, previous work (Pattingre *et al.*, 2003) has demonstrated that when AGS3 binds and keeps $G\alpha_{i3}$ inactive, an early step in autophagosome formation is triggered. Others (Gotthardt *et al.*, 2006) have also speculated that $G\alpha_{i3}$ plays an essential role early during initiation of autophagy based on proteomic studies of isolated autophagic compartments demonstrating G protein recruitment early during autophagy. Our work defines the mechanism of reversible association of $G\alpha_{i3}$ with LC3-positive, autophagosome-like membranes: AGS3 maintains inactive $G\alpha_{i3}$ on these membranes in starved cells whereas GIV activates and releases $G\alpha_{i3}$ from LC3-positive vesicles after growth factor stimulation. Because the levels of $G\alpha_{i3}$ and AGS3 proteins did not change significantly during serum starvation, with or without lysosomal protease inhibitors (unpublished data), we propose that LC3–AGS3–$G\alpha_{i3}$ complexes are unlikely to form on internal membranes that undergo lysosomal degradation during autophagy. Instead, they are likely to be formed predominantly on the outer membrane of the multilamellated autophagic bodies enriched in LC3 such that they are accessible to cytosolic GIV (Figure 7A). Because GIV was not found on immunoisolated LC3-positive membranes by us (Figure 6C) or by others using autophagosome proteomics (Garin *et al.*, 2001; Gotthardt *et al.*, 2006; Stuart *et al.*, 2007), we propose that GIV may be transiently recruited to LC3-positive membranes to release $G\alpha_{i3}$ from the membrane-bound AGS3–LC3 complexes and thereby inhibit autophagy. Although the role of inactive $G\alpha_{i3}$ in triggering autophagosome formation remains unresolved, it is possible that mammalian $G\alpha_{i3}$, much like the yeast $G\alpha$ subunit, Gpa1, binds and activates PI3K class III (Slessareva *et al.*, 2006), an enzyme activity known to be essential in autophagosome biogenesis (Meijer and Codogno, 2004).

AGS3 and GIV coordinate anti-autophagic signals from distinct locations in cells

On the basis of our results, we propose a working model (Figure 7A) and a protein–protein regulatory network (Figure 7B), both of which highlight $G\alpha_{i3}$ activity as the pivot on which levels of autophagy are reversibly balanced. Our results suggest that AGS3 and GIV exert their regulatory roles during either starvation-induced autophagy or insulin-triggered recovery by modulating $G\alpha_{i3}$ activity on LC3-positive membranes. We also demonstrate an obligate requirement of GIV's GEF motif and G protein activation in enhancement of the anti-autophagic PI3K-mTOR pathway by insulin, which is known to occur at the PM (Beugnet *et al.*, 2003; Meijer and Codogno, 2004). We propose that activation of $G\alpha_{i3}$ by GIV during insulin-mediated reversal of autophagy occurs at least at two distinct locations: on LC3-positive membranes to promote $G\alpha_{i3}$ release from AGS3–LC3 complexes and at the PM to enhance class 1 PI3K-mTOR signals triggered by growth factor receptors, as we showed in the case of EGF-triggered PI3K-Akt signals (Ghosh *et al.*, 2010). Whether these two processes occur sequentially or simultaneously and what their relative contributions are during recovery from autophagy remain to be elucidated.

In conclusion, we have integrated GIV within the signaling networks that balance the delicate equilibrium of autophagy and have described a novel molecular mechanism by which this nonreceptor GEF orchestrates reversal of autophagy by activating $G\alpha_{i3}$. The mechanistic insights gained herein not only define a new paradigm in yin-yang reversible regulation of $G\alpha$ activity by paired modulators AGS3 and GIV but also pinpoint the hitherto elusive link between the G protein, its modulators, and the autophagosome-resident molecular machinery.

MATERIALS AND METHODS

EM

Samples were processed as described in Takeda *et al.* (2001), viewed using a JEOL 1200EX II transmission electron microscope, and photographed using a Gatan Orius 600 digital camera. Pixel

size was calibrated by Pelco grating replica 607 (Ted Pella, Redding, CA) with measurements performed in ImageJ. Cells were randomly chosen using the sampling criteria that the section contained both Golgi stacks and the nucleus. Autophagosomal structures were identified as vesicles containing heterogeneous, multilamellar intraluminal material, and the numbers per cell profile were counted using these criteria. To eliminate investigator bias, samples were analyzed in a blinded manner.

Protein purification

GST, GST-Gα_{i3}, GST-LC3, GST-AGS3 (aa 465–650), His-Gα_{i3}, His-AGS3 (aa 424–650), and His-GIV-CTs (aa 1660–1870) constructs were expressed in *Escherichia coli* and purified exactly as described previously (Garcia-Marcos *et al.*, 2009, 2010). AGS3–Gα_{i3} complexes were purified after overnight incubation of GST-AGS3 with excess His-Gα_{i3} at 4°C in the presence of 10 μM GDP and 5 mM $MgCl_2$ by glutathione-Sepharose 4B affinity chromatography. After removal of excess His-Gα_{i3}, the protein complexes were eluted and buffer exchanged into G protein storage buffer and stored at −80°C. GIV–Gα_{i3} complexes were purified by incubating 40 μM His-GIV-CTs and 40 μM His-Gα_{i3} at 4°C overnight in the presence of 10 μM GDP and 5 mM $MgCl_2$ followed by gel filtration chromatography in a Superdex 200 10/300 GL column using an AKTA fast-performance liquid chromatography apparatus (GE Healthcare). The protein complexes were concentrated in G protein storage buffer using Ultracel-10K centrifugal filters (Millipore, Billerica, MA), aliquoted, and stored at −80°C.

Immunoprecipitation, in vitro binding, and displacement assays

Cell lysates (~1–2 mg protein) were incubated 4 h at 4°C with 2 μg anti-FLAG monoclonal antibody (mAb) for immunoprecipitation of Gα_{i3}-FLAG (Figure 4A and Supplemental Figure S4), anti-Gα_{i3} polyclonal antibody (pAb) (Santa Cruz Biotechnology, Santa Cruz, CA) for immunoprecipitation of endogenous Gα_{i3}, anti-HA (Covance, Princeton, NJ) for immunoprecipitation of AGS3-HA, anti-GFP mAb (Invitrogen, Carlsbad, CA) for immunoprecipitation of GFP-LC3 and immunoisolation of LC3-positive vesicles or their respective preimmune control IgGs. Protein A (for Gα_{i3} pAb) or G (for all other mAbs) agarose beads (Invitrogen) were added and incubated at 4°C for an additional 60 min. Beads were washed and then resuspended and boiled in SDS sample buffer. Buffers were supplemented with 100 μM sodium orthovanadate for all steps of the assay.

For the Gα_{i3} displacement assays, purified His-Gα_{i3} GST-AGS3 or His-Gα_{i3}:His-GIV-CT complexes were incubated with increasing amounts of His-GIV-CT or GST-AGS3 in 240 μl buffer identical to that used in the GTPase assays (20 mM Na-HEPES, pH 8, 100 mM NaCl, 1 mM EDTA, 2 mM $MgCl_2$, 1 mM dithiothreitol [DTT], 0.05% [wt/vol] C12E10 supplemented with 0.5 μM GTP) for 30 min at 30°C. Then 20 μl glutathione-agarose beads were added to the tubes and incubated for 60 min at 4°C. After extensive washing, proteins bound to the beads were eluted with sample buffer for SDS–PAGE. The experiments investigating displacement of AGS3 by GIV and vice versa were performed as previously described (Ghosh *et al.*, 2008; Garcia-Marcos *et al.*, 2009) with minor modifications. Briefly, GST-Gα_{i3} (1 μg) immobilized on glutathione-agarose beads was incubated with His-GIV-CT (6 μg) or His-AGS3 (0.1 μg) in binding buffer (50 mM Tris-HCl, pH 7.4, 100 mM NaCl, 0.4% [vol/vol] NP-40, 10 mM $MgCl_2$, 5 mM EDTA, and 2 mM DTT, supplemented with 30 μM GDP) overnight at 4°C. Samples were washed several times with binding buffer to remove the unbound His-GIV-CTs or His-AGS3 and subsequently incubated in binding buffer for 4 h at 4°C with different amounts of His-AGS3 (0, 0.02, 0.04 μM) or His-GIV-CTs (0, 1.2, 1.8 μM) as indicated. After extensive washing (4.3 mM Na_2HPO_4, 1.4 mM KH_2PO_4, pH 7.4, 137 mM NaCl, 2.7 mM KCl, 0.1% [vol/vol] Tween 20, 10 mM $MgCl_2$, 5 mM EDTA, and 2 mM DTT supplemented with 30 μM GDP), bound proteins were eluted with sample buffer for SDS–PAGE.

For the Gα_{i3}–AGS3–LC3 ternary complex experiments, GST pull-down assays were carried out as previously described (Ghosh *et al.*, 2008; Garcia-Marcos *et al.*, 2009) with minor modifications. Purified GST-LC3 (15–20 μg) or GST alone (30 μg) was immobilized on glutathione-Sepharose beads and incubated at 4°C overnight in binding buffer (50 mM Tris-HCl, pH 7.4, 100 mM NaCl, 0.4% [vol/vol] NP-40, 10 mM $MgCl_2$, 5 mM EDTA, 2 mM DTT, and 30 μM GDP) containing His-AGS3, His-Gα_{i3}, or a 1:3 ratio of His-AGS3:His-Gα_{i3}. The following day, the excess unbound AGS3 and Gα_{i3} proteins were removed by washing, and the GST–LC3-bound complexes resuspended in binding buffer with increasing amounts (0, 2, and 6 μg) of His-GIV-CTs WT or F1685A mutant. After incubation at 4°C for 4 h, the beads were washed (4.3 mM Na_2HPO_4, 1.4 mM KH_2PO_4, pH 7.4, 137 mM NaCl, 2.7 mM KCl, 0.1% [vol/vol] Tween 20, 10 mM $MgCl_2$, 5 mM EDTA, 2 mM DTT, and 30 μM GDP), and bound proteins were eluted in sample buffer for SDS–PAGE.

Immunofluorescence on whole cell and semithin cryosections

Cells were fixed at room temperature with 3% paraformaldehyde for 20–25 min, permeabilized (0.2% Triton X-100) for 45 min, and incubated for 1 h each with primary and then secondary antibodies as described previously (Ghosh *et al.*, 2008). Antibody dilutions were as follows: affinity-purified AGS3 pAb, 1:250; GFP mAb, 1:1000; affinity-purified pAb LC3, 1:100; secondary goat anti–rabbit (594) and goat anti–mouse (488) Alexa-conjugated antibodies, 1:500; and 4′,6-diamino-2-phenylindole (DAPI), 1:2000 (Invitrogen). Samples were examined with a Zeiss Axiophot microscope (Carl Zeiss, Thornwood, NY) using a 63 × 1.30 numerical aperture (NA) (Zeiss Plan Neofluar), and images were collected with the ORCA-ER camera (Hamamatsu, Bridgewater, NJ) and Volocity Software. All individual images were processed using ImageJ software (National Institutes of Health, Bethesda, MD) and assembled for presentation using Photoshop and Illustrator software (both Adobe).

For immunofluorescence on semithin cryosections, sections (0.5–1 μm) were cut with a Leica Ultracut UCT microtome equipped with a FCS cryoattachment (Fukasawa *et al.*, 2009) at −100°C and incubated with primary antibodies overnight at 4°C followed by detection with Alexa 594 goat anti–rabbit and 488 goat anti–mouse IgG in phosphate-buffered saline containing 5% FCS for 2 h at room temperature. Samples were examined, and images were captured as above.

For colocalization of AGS3 with GFP-LC3, HeLa cells were starved for 8 h in 0.2% FBS/DMEM, supplemented with lysosomal inhibitors (10 μg/ml leupeptin and pepstatin) (Sigma), permeabilized with 0.05% saponin (Sigma) for 50 s at 25°C before fixation, and processed for immunofluorescence as above. Cells were analyzed by confocal microscopy using 60× PlanApo N objective lenses (NA 1.42, oil immersion) on an inverted Olympus FluoView 1000 confocal microscope. The microscope was equipped with DAPI (405 nm excitation, 430–470 emission), Alexa-488 (488 excitation, 505/525 emission), Alexa-594 (543 excitation, 560/620 emission), and Alexa-647 (635 excitation, 655–755 emission) filter sets; a manual stage; and a Photometrics

(Tucson, AZ) CH350 CCD camera (Hamamatsu). All individual images were processed using ImageJ software and assembled for presentation using Photoshop and Illustrator software.

Subcellular fractionation and immunoisolation of GFP-LC3–positive vesicles

LC3-positive membranes were immunoisolated as described (Gao *et al.*, 2010) with modifications. Cells expressing GFP-LC3 were harvested at 48 h posttransfection, suspended in homogenization buffer (10 mM sodium phosphate buffer [pH 7.2], 1 mM $MgCl_2$, 30 mM NaCl, 1 mM DTT, and 0.5 mM phenylmethylsulfonyl fluoride, supplemented with protease and phosphatase inhibitors), and homogenized using a 30-gauge needle. Crude membranes from the homogenate were pelleted by centrifugation of postnuclear supernatant at 100,000 × *g* for 60 min at 4°C in a TLA-41 fixed-angle rotor in a TLA-100 table-top ultracentrifuge (Beckman Coulter, Krefeld, Germany). Pelleted membranes were washed twice in homogenization buffer before resuspension. Autophagosomes were immunoisolated on protein G agarose beads using GFP mAb, washed with homogenization buffer, and eluted by boiling in SDS sample buffer. The purity of the autophagosomal isolation was assessed by immunoblotting for organelle markers: early endosomes (EEA1), endoplasmic reticulum–Golgi (calnuc and βCOP), PM and recycling endosomes (transferrin receptor), lamin A (nucleus), and lysosomes (cathepsin D).

Creation of protein–protein interaction map

The protein–protein interaction map was based on interactions listed in the I2D database (Brown and Jurisica, 2005; Brown *et al.*, 2009) and functional interactions that were validated in the literature. For simplicity it was restricted mainly to functional interactions between proteins and signaling pathways relevant to autophagy, G protein, and growth factor signaling. The layout of the map was designed using NAViGaTOR software (http://ophid.utoronto.ca/navigator).

Other methods

Steady-state GTPase assays were performed exactly as described previously (Garcia-Marcos *et al.*, 2009, 2010). Detailed information on reagents and antibodies, plasmids and mutagenesis, cell culture, and transfection are provided in the Supplemental Materials.

ACKNOWLEDGMENTS

We thank Gordon N. Gill (University of California, San Diego [UCSD]). for thoughtful comments during preparation of the manuscript, Yelena Pavlova and Karen Sykes for assistance with cell culture and other technical support, and Karla Kirkegaard (Stanford) and Catherine Denicourt (University of Tennessee Health Science Center) for GST- and GFP-tagged LC3 constructs, respectively. We also thank the UCSD School of Medicine Light Microscopy Facility, supported in part by National Institute of Neurological Disorders and Stroke P30 NS-047101 and National Institute of Diabetes and Digestive and Kidney Diseases DK-80506, and its director, Jennifer Meerloo. This work was funded by the Career Awards for Medical Scientists (Burroughs Wellcome Fund). and Research Scholar (American Gastroenterology Association FDN) awards to P.G. and National Institutes of Health grant DK-I7780 to M.G.F. M.G.-M. was supported by Susan G. Komen postdoctoral fellowship KG080079. Jason Ear was supported by the UCSD McNair Scholarship Program.

REFERENCES

Adhikari A, Sprang SR (2003). Thermodynamic characterization of the binding of activator of G protein signaling 3 (AGS3). and peptides derived from AGS3 with $G\alpha_{i1}$. J Biol Chem 278, 51825–51832.

Beugnet A, Tee AR, Taylor PM, Proud CG (2003). Regulation of targets of mTOR (mammalian target of rapamycin). signalling by intracellular amino acid availability. Biochem J 372, 555–566.

Brown KR, Jurisica I (2005). Online predicted human interaction database. Bioinformatics 21, 2076–2082.

Brown KR, Otasek D, Ali M, McGuffin MJ, Xie W, Devani B, Toch IL, Jurisica I (2009). NAViGaTOR: Network Analysis, Visualization and Graphing Toronto. Bioinformatics 25, 3327–3329.

Cao C, Huang X, Han Y, Wan Y, Birnbaumer L, Feng GS, Marshall J, Jiang M, Chu WM (2009). $G\alpha_{i1}$ and $G\alpha_{i3}$ are required for epidermal growth factor–mediated activation of the Akt-mTORC1 pathway. Sci Signal 2, ra17.

Cecconi F, Levine B (2008). The role of autophagy in mammalian development: cell makeover rather than cell death. Dev Cell 15, 344–357.

De Vries L, Fischer T, Tronchere H, Brothers GM, Strockbine B, Siderovski DP, Farquhar MG (2000). Activator of G protein signaling 3 is a guanine dissociation inhibitor for $G\alpha_i$ subunits. Proc Natl Acad Sci USA 97, 14364–14369.

Fukasawa H, Bornheimer S, Kudlicka K, Farquhar MG (2009). Slit diaphragms contain tight junction proteins. J Am Soc Nephrol 20, 1491–1503.

Gao W, Kang JH, Liao Y, Ding WX, Gambotto AA, Watkins SC, Liu YJ, Stolz DB, Yin XM (2010). Biochemical isolation and characterization of the tubulovesicular LC3-positive autophagosomal compartment. J Biol Chem 285, 1371–1383.

Garcia-Marcos M, Ghosh P, Ear J, Farquhar MG (2010). A structural determinant that renders $G\alpha_i$ sensitive to activation by GIV/girdin is required to promote cell migration. J Biol Chem 285, 12765–12777.

Garcia-Marcos M, Ghosh P, Farquhar MG (2009). GIV is a nonreceptor GEF for $G\alpha_i$ with a unique motif that regulates Akt signaling. Proc Natl Acad Sci USA 106, 3178–3183.

Garin J, Diez R, Kieffer S, Dermine JF, Duclos S, Gagnon E, Sadoul R, Rondeau C, Desjardins M (2001). The phagosome proteome: insight into phagosome functions. J Cell Biol 152, 165–180.

Ghosh P *et al.* (2010). A Gi-GIV molecular complex binds epidermal growth factor receptor and determines whether cells migrate or proliferate. Mol Biol Cell 20, 2338–2354.

Ghosh P, Garcia-Marcos M, Bornheimer SJ, Farquhar MG (2008). Activation of $G\alpha_{i3}$ triggers cell migration via regulation of GIV. J Cell Biol 182, 381–393.

Gilman AG (1987). G proteins: transducers of receptor-generated signals. Annu Rev Biochem 56, 615–649.

Gohla A, Klement K, Piekorz RP, Pexa K, vom Dahl S, Spicher K, Dreval V, Haussinger D, Birnbaumer L, Nurnberg B (2007). An obligatory requirement for the heterotrimeric G protein G_{i3} in the antiautophagic action of insulin in the liver. Proc Natl Acad Sci USA 104, 3003–3008.

Gotthardt D, Blancheteau V, Bosserhoff A, Ruppert T, Delorenzi M, Soldati T (2006). Proteomics fingerprinting of phagosome maturation and evidence for the role of a Gα during uptake. Mol Cell Proteomics 5, 2228–2243.

Jiang P, Enomoto A, Jijiwa M, Kato T, Hasegawa T, Ishida M, Sato T, Asai N, Murakumo Y, Takahashi M (2008). An actin-binding protein Girdin regulates the motility of breast cancer cells. Cancer Res 68, 1310–1318.

Kimple RJ, Kimple ME, Betts L, Sondek J, Siderovski DP (2002). Structural determinants for GoLoco-induced inhibition of nucleotide release by Gα subunits. Nature 416, 878–881.

Kimura S, Fujita N, Noda T, Yoshimori T (2009). Monitoring autophagy in mammalian cultured cells through the dynamics of LC3. Methods Enzymol 452, 1–12.

Kitamura T *et al.* (2008). Regulation of VEGF-mediated angiogenesis by the Akt/PKB substrate Girdin. Nat Cell Biol 10, 329–337.

Klionsky DJ *et al.* (2008). Guidelines for the use and interpretation of assays for monitoring autophagy in higher eukaryotes. Autophagy 4, 151–175.

Krumins AM, Gilman AG (2006). Targeted knockdown of G protein subunits selectively prevents receptor-mediated modulation of effectors and reveals complex changes in nontargeted signaling proteins. J Biol Chem 281, 10250–10262.

Levine B, Kroemer G (2008). Autophagy in the pathogenesis of disease. Cell 132, 27–42.

Lum JJ, DeBerardinis RJ, Thompson CB (2005). Autophagy in metazoans: cell survival in the land of plenty. Nat Rev Mol Cell Biol 6, 439–448.

Meijer AJ, Codogno P (2004). Regulation and role of autophagy in mammalian cells. Int J Biochem Cell Biol 36, 2445–2462.
Mizushima N, Yoshimori T (2007). How to interpret LC3 immunoblotting. Autophagy 3, 542–545.
Ogier-Denis E, Couvineau A, Maoret JJ, Houri JJ, Bauvy C, De Stefanis D, Isidoro C, Laburthe M, Codogno P (1995). A heterotrimeric G_{i3}-protein controls autophagic sequestration in the human colon cancer cell line HT-29. J Biol Chem 270, 13–16.
Ogier-Denis E, Houri JJ, Bauvy C, Codogno P (1996). Guanine nucleotide exchange on heterotrimeric G_{i3} protein controls autophagic sequestration in HT-29 cells. J Biol Chem 271, 28593–28600.
Ogier-Denis E, Pattingre S, El Benna J, Codogno P (2000). Erk1/2-dependent phosphorylation of Gα-interacting protein stimulates its GTPase accelerating activity and autophagy in human colon cancer cells. J Biol Chem 275, 39090–39095.
Ogier-Denis E, Petiot A, Bauvy C, Codogno P (1997). Control of the expression and activity of the Gα-interacting protein (GAIP). in human intestinal cells. J Biol Chem 272, 24599–24603.
Pattingre S, De Vries L, Bauvy C, Chantret I, Cluzeaud F, Ogier-Denis E, Vandewalle A, Codogno P (2003). The G-protein regulator AGS3 controls an early event during macroautophagy in human intestinal HT-29 cells. J Biol Chem 278, 20995–21002.
Peterson YK, Bernard ML, Ma H, Hazard S III, Graber SG, Lanier SM (2000). Stabilization of the GDP-bound conformation of Giα by a peptide derived from the G-protein regulatory motif of AGS3. J Biol Chem 275, 33193–33196.
Shintani T, Klionsky DJ (2004). Autophagy in health and disease: a double-edged sword. Science 306, 990–995.
Slessareva JE, Routt SM, Temple B, Bankaitis VA, Dohlman HG (2006). Activation of the phosphatidylinositol 3-kinase Vps34 by a G protein α subunit at the endosome. Cell 126, 191–203.
Stuart LM *et al.* (2007). A systems biology analysis of the *Drosophila* phagosome. Nature 445, 95–101.
Takeda T, McQuistan T, Orlando RA, Farquhar MG (2001). Loss of glomerular foot processes is associated with uncoupling of podocalyxin from the actin cytoskeleton. J Clin Invest 108, 289–301.
Tall GG, Gilman AG (2005). Resistance to inhibitors of cholinesterase 8A catalyzes release of $G\alpha_i$-GTP and nuclear mitotic apparatus protein (NuMA). from NuMA/LGN/$G\alpha_i$-GDP complexes. Proc Natl Acad Sci USA 102, 16584–16589.
Thomas CJ, Tall GG, Adhikari A, Sprang SR (2008). Ric-8A catalyzes guanine nucleotide exchange on $G\alpha_{i1}$ bound to the GPR/GoLoco exchange inhibitor AGS3. J Biol Chem 283, 23150–23160.
von Mering C, Jensen LJ, Snel B, Hooper SD, Krupp M, Foglierini M, Jouffre N, Huynen MA, Bork P (2005). STRING: known and predicted protein–protein associations, integrated and transferred across organisms. Nucleic Acids Res 33, D433–D437.
Wang J, Whiteman MW, Lian H, Wang G, Singh A, Huang D, Denmark T (2009). A noncanonical MEK/ERK signaling pathway regulates autophagy via regulating Beclin 1. J Biol Chem 284, 21412–21424.
Willard FS, Kimple RJ, Siderovski DP (2004). Return of the GDI: the GoLoco motif in cell division. Annu Rev Biochem 73, 925–951.
Yanamadala V, Negoro H, Denker BM (2009). Heterotrimeric G proteins and apoptosis: intersecting signaling pathways leading to context dependent phenotypes. Curr Mol Med 9, 527–545.